

ON THE SYSTEMATIC POSITION OF THE MOSS GENUS *CATOSCOPIUM*,  
WITH A NEW APPROACH TO THE PERISTOME REDUCTION STUDY

О СИСТЕМАТИЧЕСКОМ ПОЛОЖЕНИИ МХОВ РОДА *CATOSCOPIUM*,  
С ОБСУЖДЕНИЕМ НОВОГО ПОДХОДА К ИЗУЧЕНИЮ РЕДУКЦИИ ПЕРИСТОМА

MICHAEL S. IGNATOV<sup>1</sup>, ULYANA N. SPIRINA<sup>1,2</sup>, ELENA A. IGNATOVA<sup>3</sup>,  
MICHAEL KRUG<sup>4</sup> & DIETMAR QUANDT<sup>4</sup>

МИХАИЛ С. ИГНАТОВ<sup>1</sup>, УЛЬЯНА Н. СПИРИНА<sup>1,2</sup>, ЕЛЕНА А. ИГНАТОВА<sup>3</sup>,  
МИХАИЛ КРУГ<sup>4</sup>, ДИТМАР КВАНДТ<sup>4</sup>

Abstract

The early stages of the peristome development in the monospecific moss genus *Catoscopium* were studied. The peristomial formula 4:2:3 is the most common, although there are deviations, increasing in number at later stages of development. Additional cell divisions were observed in all peristomial layers, as well as an “under-performance” of unequal cell divisions, resulting in the formula 4:2:4-opposite. The most commonly observed 4:2:3 pattern does not contradict the placement of *Catoscopium* among haplolepidous mosses, but at the same time it does not necessarily confirm this placement, because the 4:2:3 pattern appears to be present in basal arthroodontous mosses, and is not so rare in diplolepidous alternate mosses at the early stages. The latter was found in *Podperaea*, a hypnlean moss with only slightly reduced “perfect” peristome, involved in the present study for comparison for trait comparisons with *Catoscopium*. Likewise, the formula 4:2:4-opposite appears in unrelated phylogenetic lineages, being in many cases associated with various patterns of morphological reduction. Phylogenetic analysis based on four mitochondrial (*cob1420*, *nad2* with *nad2i156*, *nad5* with *nad5i753*, *nad5-nad4* IGS) and three plastid (*rbcL*, *rps4*, *trnL* G1) markers is performed, indicating the position of *Catoscopium* in relation to groups with 4:2:3 and 4:2:4-opposite and 4:2:4-alternate peristomial formulae. A method of total peristome structure visualization by the RGB-coded schemes of the total capsule circumference is introduced.

Резюме

Изучены ранние стадии развития перистома монотипного рода *Catoscopium*, систематическое положение которого трактовалось разными авторами различно. Формула перистома 4:2:3 наиболее часто встречается у *Catoscopium* на ранних стадиях развития спорофита, однако отклонения от нее многочисленны, и их число возрастает на более поздних стадиях. При этом во всех слоях клеток, участвующих в образовании перистома, наблюдаются как дополнительные деления клеток, так и “недопредставленность неравных клеточных делений”, обуславливающих образование формулы 4:2:3, что приводит к образованию 4:2:4-супротивному типу. Такое строение согласуется с положением *Catoscopium* в филогенетических деревьях в основании клады, образованной гаплотепидными группами, но в то же время не является строго специфичным для такого решения, поскольку 4:2:3 иногда встречается и в наиболее базальных группах артродонтных мхов, а также она представлена и на ранних стадиях развития диплотепидных-очередных групп, что иллюстрируется в статье на примере рода *Podperaea*, представителя Нурпалес, с весьма незначительно редуцированным перистомом, близким по строению к “полно развитому” типу. *Podperaea* была включена в анализ для сравнения с *Catoscopium*, степень редукции перистома которого значительно сильнее. Отмечается, что формула 4:2:4 с супротивным расположением элементов перистома появляется в разных филогенетических линиях, в большинстве случаев связанных с редукцией перистома. Обсуждение их филогенетического положения проведено на основе анализа по 4 митохондриальным (*cob1420*, *nad2* with *nad2i156*, *nad5* with *nad5i753*, *nad5-nad4* IGS) и трем хлоропластным (*rbcL*, *rps4*, *trnL* G1) участкам генома. Предложен метод представления полной структуры перистома с помощью развертки с использованием RGB-кодировки.

KEYWORDS: bryophytes, phylogeny, morphology, peristome, haplolepidous, unequal cell divisions

<sup>1</sup> – Tsitsin Main Botanical Garden of Russian Academy of Sciences, Botanicheskaya 4, Moscow 127276 Russia; e-mail: misha\_ignatov@list.ru

<sup>2</sup> – Biological Faculty, Tver State University, Zhelyabova 33, Tver 170100 Russia; e-mail: ulayspirina@mail.ru

<sup>3</sup> – Biological Faculty, Moscow State University, Moscow 119991 Russia; e-mail: arctoa@list.ru

<sup>4</sup> – Nees-Institut für Biodiversität der Pflanzen Rheinische, Friedrich-Wilhelms-Universität, Meckenheimer Allee 170 D-53115 Bonn, Germany; e-mails: mkrug@uni-bonn.de, quandt@uni-bonn.de

## INTRODUCTION

Recent advances in the molecular phylogenetic studies have resulted in a number of unexpected and surprising misplacements in many groups of living beings. The general pattern is that in groups with low levels of morphological diversity, systematic reevaluations from molecular data tend to be most numerous. In mosses many genera were transferred to other families, and relationships of many families were reevaluated against traditional classifications (Newton *et al.*, 2000; Ignatov *et al.*, 2007; Goffinet *et al.*, 2009; Olsson *et al.*, 2009; Huttunen *et al.*, 2012a; Stech *et al.*, 2012). This is especially true for taxa with reduced peristomes (compare Huttunen *et al.*, 2012b), the complex organ of spore release in mosses, which provides the basis for most moss classifications. For example, the genus *Archidium*, previously considered extremely primitive and placed in a separate subclass (Snider, 1975a,b; Crum & Anderson, 1981), appeared to be nested in the haplolepidous clade (Newton *et al.*, 2000; Cox *et al.*, 2004; Stech *et al.*, 2012). At the same time, *Oedipodium*, traditionally placed in or near the Splachnaceae, appears to be sister to all Bryalean moss groups with transverse capsule dehiscence (Shaw & Renzaglia, 2004; Goffinet *et al.*, 2009), and probably it is even primarily eperistomate (Shimamura & Deguchi, 2008; Hyvönen *et al.*, 2004). Similarly, once no sporophyte is known at all the systematic placement of the taxon is often controversial, especially in the presence of non-conclusive gametophytic characters. A remarkable example represents *Pulchrinodus* which has been placed all over the moss tree of life (compare Allen, 1987) until molecular studies revealed its placement at the base of the Bryales (Quandt *et al.*, 2007). There are however opposite examples, where peristomes have complex structures allowing different interpretations of their phylogenetic origin, *e.g.*, in Timmiales. Their phylogenetic position among early diverging arthodontous mosses became apparent only after molecular phylogenetic analyses (*e.g.* Newton *et al.*, 2000; Cox *et al.*, 2004; Wahrmond *et al.*, 2010) and subsequent developmental studies resulted in reinterpretations of the peristome morphology in light of the different phylogenetic hypotheses (Budke *et al.*, 2007).

The genus *Catoscopium*, with a single circumpolar mire species *C. nigratum* (Hedw.) Brid., was originally classified in the Meesiaceae (Schimper, 1860; Limpricht, 1895), but was later placed in its own family although still next to Meesiaceae (Brotherus, 1924; Podpera, 1954). An alternative placement has been suggested by Griffin & Buck (1989), who referred *Catoscopium* to Bartramiaceae. These classification decisions were based on weak morphological evidence due to considerable peristome reduction in *Catoscopium*: the exostome teeth are irregular, although they still have a distinct median line, while the endostome is represented by a poorly developed basal membrane, not allowing a clear understanding of the

position of its parts relative to the exostome teeth (Figs. 1-2). However, diplolepidous peristomes at various stages of reduction are common in both Bartramiaceae and Meesiaceae, and this fact may explain the placement of *Catoscopium* near or within these families. Even in more recent treatments its position is a rather controversial one. While in Buck & Goffinet (2000) it is found within the Splachnales, Goffinet *et al.* (2009) place it in the Bryales. In contrast Ignatov & Ignatova (2003) accepted *Catoscopium* in a separate order among early diverging arthodontous mosses. Similarly, recent molecular analyses reported *Catoscopium* among early diverging haplolepidous mosses (Quandt *et al.*, 2007; Wahrmond *et al.*, 2010), a view shared by Frey & Stech (2009). However a detailed discussion on its morphology was never provided, partly due to a partial peristome reduction (Fig. 1A-C), precluding an easy approach to understanding its morphology.

Peristomes play a considerable adaptive role in spore release (Shaw & Robinson, 1984), and in more than 95% of species they belong to an advanced arthodontous type. Peristomes of this type are usually developed from three rings of cells that partly decompose and form from retained material in two rows of peristomial elements. Adjoining material of the inner cell walls of the outer peristomial layer (OPL) and outer cell walls of the middle, or primary peristomial layer (PPL) form the outer ring of teeth, the exostome, while cell walls between the PPL and inner peristomial layer (IPL) build another ring, the endostome, usually composed of a more delicate structure. Edwards (1979) introduced the peristomial formula, counting cells in these three layers for 1/8 of sporophyte circumference.

Three types of arthodontous peristomes are usually recognized as the main ones (Shaw & Robinson, 1984; Edwards, 1984) and recently they appeared to be quite congruent with the molecular phylogenetic results (*e.g.*, Shaw *et al.*, 2003; Tsubota *et al.*, 2004; Shaw & Renzaglia, 2004; Cox *et al.*, 2010; Wahrmond *et al.*, 2010; Shaw *et al.*, 2011). These are haplolepidous, diplolepidous-opposite and diplolepidous-alternate peristomes (Fig. 3).

Their difference among peristome types becomes apparent at an early stage of differentiation in the peristomial layers, when the IPL undergoes a division which turns it from 8-celled to 16-celled. At the stage when the 2:2:1 pattern is transforming into 4:2:2, the divisions in IPL can be:

- 1) aligned with the anticlinal cell walls in the PPL, resulting in the diplolepidous-opposite, or “*Funaria*”-type, with variants 4:2:2, 4:2:4 or 4:2:8;
- 2) offset to anticlinal cell walls in the PPL and with one subsequent division of the larger cell, resulting in haplolepidous, or “*Dicranum*”-type, 4:2:3;
- 3) offset to anticlinal cell walls in the PPL, with 2-6 subsequent divisions in IPL and misplacing of the previ-

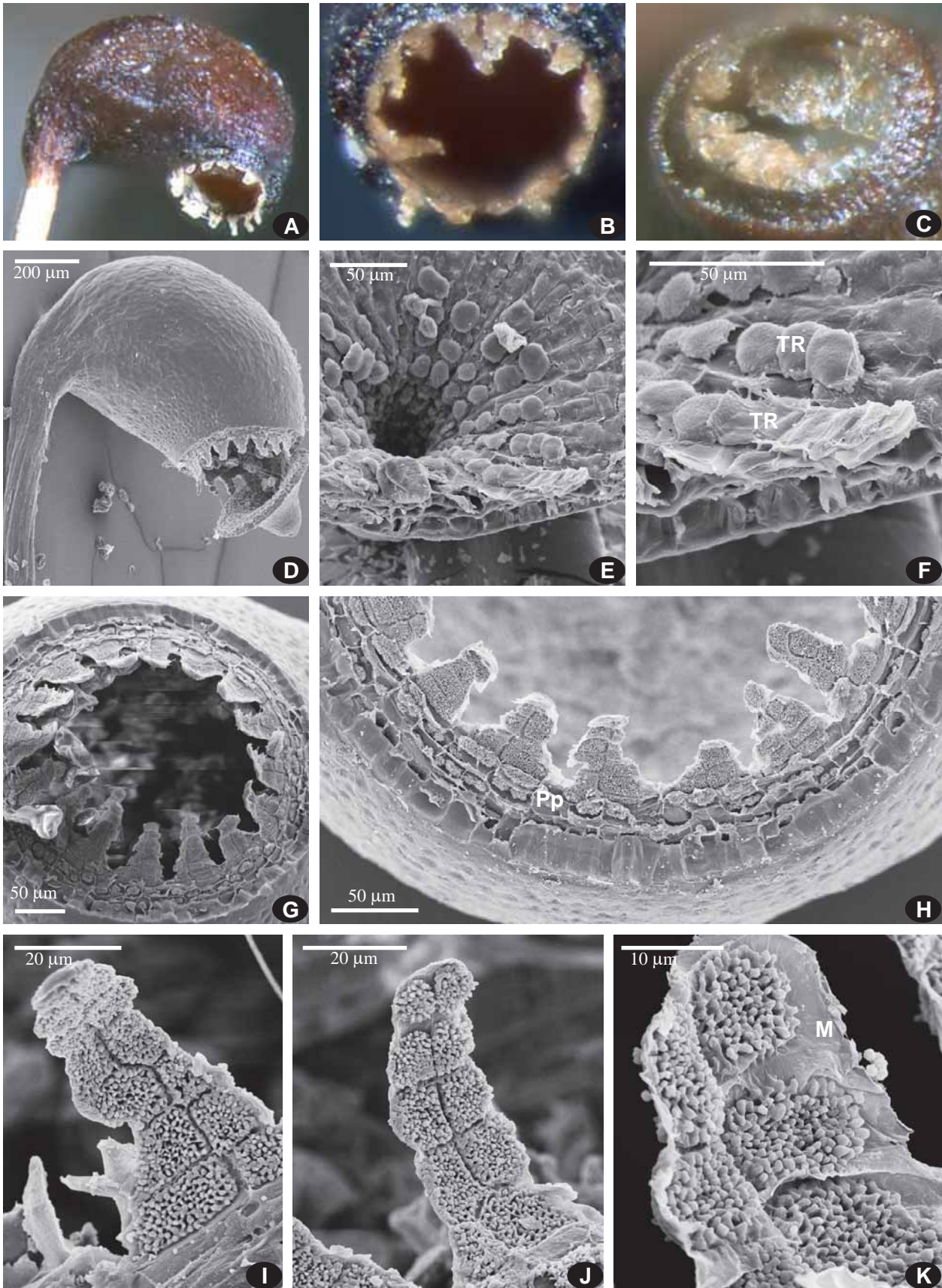


Fig. 1. *Catoscopium nigritum*, peristomes under stereomicroscope (A–C) and SEM (D–K) from Yakutia (A–C) and Italy (D–K): A–D, capsule mouths with peristomes; E–F, operculum with attached exostome teeth remnants (TR); G–H, exostome teeth, showing variation and preperistome; I–K, ornamentation of dorsal surface of exostome teeth, showing presence (K) or absence of margin (M).

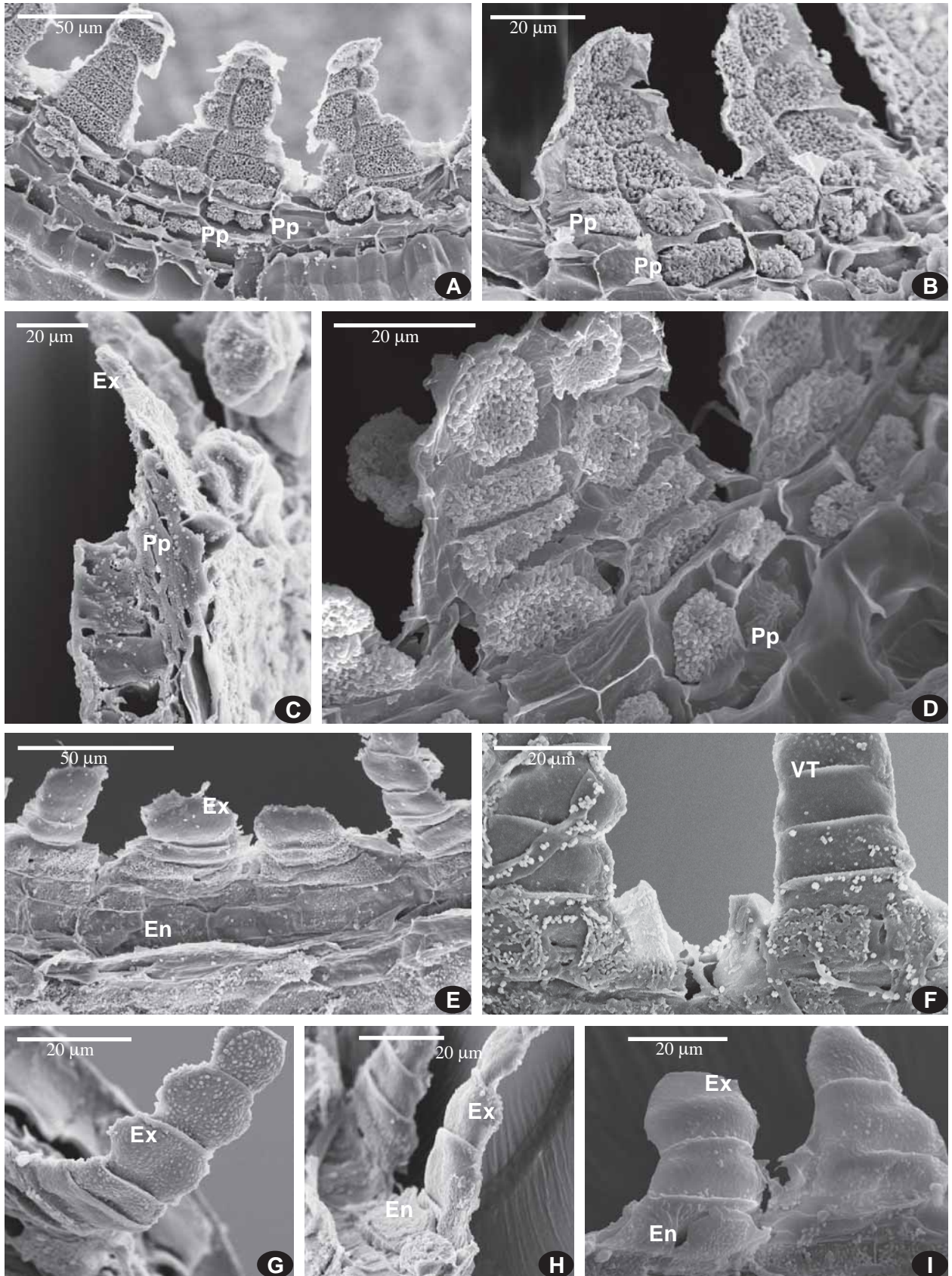
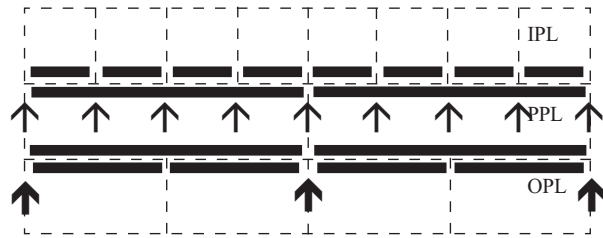
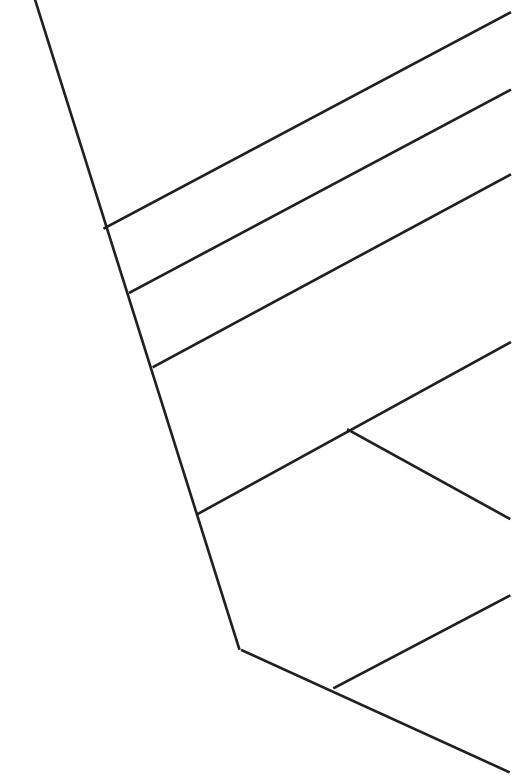
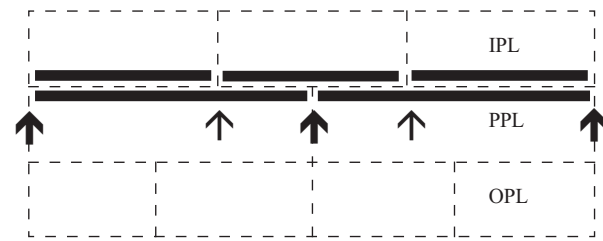


Fig. 2. *Catoscopium nigratum*, SEM images of peristome; specimens from Italy (A–C, E–H) and Arkhangelsk (D, I). A–B, D, peristome from outside, showing properistome presence (Pp); C, longitudinal section, showing exostome tooth and properistome layers at its base; E–I, peristome from inside: mostly exostome is visible (Ex), and only at places a thin membrane of endostome is discernible (En); some teeth have ventral trabeculae (VT), which are more commonly absent.

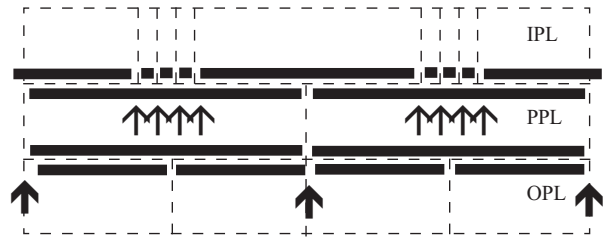
Primary eperistomate (*Sphagnum*, *Andreaea*, *Takakia*, etc.) and nematodontous (*Polytrichum*, *Tetraphis*, *Buxbaumia*)



Timmiales: 4:2:8 opposite  
[Funariaceae (4:2:2 opp., or 4:2:4 at base), Encalyptaceae (4:2:4 opp.), Disceliaceae (4:2:4, opp.)]



Dicranales, Grimmiales: 0:2:3



Bryales, Hypnales: 4:2:8 alternate  
variants include 4:2:4, 6, 8, 10, 12, 14

Fig. 3. Scheme of the main clades and main types of peristome structure.

ously aligned or nearly aligned anticlinal cell walls simultaneous with PPL cell enlargement, resulting in diplolepeideous-alternate, or “*Bryum*”-type, with variants 4:2:4, 4:2:6, 4:2:8, or more rarely 4:2:10 and as an exception 4:2:12 and 4:2:14.

This scheme with three main peristome types is based on careful studies of peristome development done for a number of genera (Evans & Hooker, 1913; Wenderoth, 1931; Saito & Shimoze, 1955; Saito, 1956; Stone, 1961; Edwards, 1979, 1984; Shaw & Anderson, 1988; Shaw & Allen, 1985; Shaw *et al.*, 1987, 1989a,b; Budke *et al.* 2007). However there are also a number of exceptions, observed both within a single cross-section and in species with peristome structure different from “typical” for families where they belong. For example, Magill (1987) found a diplolepeideous-opposite peristome in *Dichelodontium* (Ptychomniales: Hypnanae), instead of diplolepeideous-alternate. *Splachnum* and *Tetraplodon* were shown to have opposite 4:4:4 and 4:2:8 cases, respectively (Schwarz, 1994), although their position in the “diplolepeideous-alternate” clade has been confirmed in all recent molecular phylogenies cited above. Schwarz (1994) found that the peristome of *Ephemerum* has an opposite (0):4:4 structure, despite that this genus is a

member of the haplolepeideous clade, where 4:2:3 is the basic formula. The 4:2:3 formula was noted for *Aulacomnium heterostichum* (Blomquist & Robertson, 1941), although Shaw *et al.* (1989b) criticized their interpretation of cell arrangement as being incomplete. The genus *Glyphomitrium*, despite being resolved in the haplolepeideous clade (Cox *et al.*, 2010), always has an unstable proportion of IPL and PPL cells (Estébanez *et al.*, 2006).

Examination of illustrations in almost all publications, in fact, always reveals “mistakes in divisions” among “typical” patterns, *i.e.* those are most common among the other parts of the same section, and other sections of the same capsule, which usually agree with its systematic position supported by phylogenetic evidence. For example, Shaw *et al.* (1987) in Fig. 14 for *Diphyscium*, illustrate in different octants of the same section proportions of 4:2:3, 4:2:3, 4:3:4, 4:2:4, 4:2:3, 4:2:3, 4:2:3\*, 6:3:4. The octants marked here with asterisk have an offsetted IPL in the fashion characteristic for diplolepeideous-alternate peristomes: IPL anticlinal cell walls are displaced relative to anticlinal walls in both the PPL and OPL. Figure 8 in Goffinet *et al.* (1999) of *Schlotheimia rugifolia* (Hook.) Schwägr. has octants 4:2:4, 4:2:3, 4:2:4, 4:2:4, 4:2:3, 4:2:4, 4:2:3, 4:2:2.

To avoid a subjective evaluation of the anticlinal cell positions, Budke *et al.* (2007) suggested a quantitative method. It proved that the complex peristome of *Timmia* belongs to the opposite type in IPL versus PPL arrangement with great confidence, as 96% of cell walls were found to be aligned, and only 4% offset (and in all cases only slightly shifted, for less than 33% along periclinal cell wall, and never more than that).

However, a preliminary study of *Catoscopium* revealed a frequent co-occurrence of both 4:2:3 and 4:2:4 patterns within the same cross section. Thus we undertook an expanded analysis of whole series of peristome sections to answer two questions:

- 1) is it possible to recognize the basic peristome formula in the irregularly developed peristome of *Catoscopium*, and to identify its affinity to basic peristome types;
- 2) which kind(s) of division errors and displacements are associated with peristome reduction in this species.

#### MATERIALS AND METHODS

##### *General peristome morphology*

Peristomes of the *Catoscopium* were studied and photographed under light stereo- and compound microscopes, and SEM LEO-430, after gold coating but without other preparation (Fig. 1-2). Specimens used for these observations were taken from MHA herbarium, with sampling from Northern Europe (Arkhangelsk Province, Kumichevo, Ignatov, 4.VIII.1988), Caucasus (Georgia, Abramova, Exsiccate of LE #78), and Asia (Altai, Ignatov & Ignatova 12-492; Taimyr, Fedosov 08-72; Yakutia, Teply Klyuch, Ignatov & Ivanov, 6.VII.1912). One specimen from Southern Europe (Italy, Prov. Bozen: Pustertal, Dolomiten, Pragser Wildsee, Schäfer-Verwimp 27558) was also used for SEM observations.

As preliminary observations did not reveal any marked differences between populations, possible heterogeneity of the studied plants was not further considered.

##### *Anatomy study*

The material for this study was collected in Yakutia (voucher Yakutia, Tomponsky Distr., Teply Klyuch, 6.VII.2011, Ignatov & Ivanov #11-2042, MHA), in a rich fen. Young sporophytes 3-5 mm long were fixed in 4% glutaraldehyde in 2.5% Na-phosphate buffer, pH 6.8, and stored in it. After storage at +4°C, they were post-fixed with 1% osmium tetroxide in the same buffer for 10 h, then dehydrated in 70% ethanol, and then dehydrated through a graded ethanol/acetone series to 100% acetone. After that, samples were embedded in araldite 6005 medium, according to the protocol of manufacturer.

A preliminary study revealed that at the stage when peristomial layers became apparent, it is difficult to determine a peristome formula because adjacent octants have inconsistent patterns: 4:2:3, 4:2:4 aligned, 4:2:4 opposite, and occasionally cases with higher numbers of cells. The PPL in some capsules was composed of 20-22 cells, not 16. To obtain a more reliable quantitative data, we decided to check not an individual section or few best

“typical” sections, but instead the whole series, allowing a study of peristomial layer structure throughout one young sporophyte. For this purpose we cut the young sporophyte in thinner sections, 2 µm (not 5-8 µm, as commonly used in similar studies), to obtain thinner cell wall views and thus to reduce possible noise. Sections were cut with glass knives and put on glass slides without mounting medium. All sections were arranged sequentially on a slide glass, which allows finding the precise distance of each section from the level where regular peristomial structure becomes apparent (Fig. 4A, C-F).

Two capsules were cut longitudinally (Fig. 4A, B) and ten transversely, the latter with series of 30 to 130 sections, 2 µm thick. Thus 60 to 260 µm intervals were included in the study. Among them, two series included a very homogeneous cell arrangement, without obvious peristomial layers (Fig. 4G). It seems that they comprise sporophytes that did not reach a fully developed state, appearing similar to that shown in Fig. 1C, which occasionally occurs in *Catoscopium* collections.

One series was started from four cells of the so-called fundamental cross, surrounded by 1-2 rings of amphithelial cells, so the formula was 0:1. Early stages where only two peristomial layers occur, [-]:2:1, were seen in two series (Fig. 4C). Four series represent stages starting from 2:2:1 in the upper part, and with the transition to 4:2:2 shortly below. Further below, from ca. 100-120 µm from the level where regular peristomial structure becomes recognizable, the PPL was represented by 17-24 cells, rarely more, and it is likely situated at about the capsule mouth or somewhat below it (Fig. 4F).

The sectioning was done from the sporophyte apex, whereas the interval with differentiated peristomial layers was the focus of the present study. It is visible in the longitudinal section (Fig. 4A) between the arrows, as we can conclude from a comparison of sections, including their number (distance from upper to lower one in the series) and also from the width of the peristomial layers.

As cell walls appeared to be obscured by collapsed cytoplasm under the light microscope, we conducted observations by means of fluorescence of cell walls stained by berberin and photographed under confocal LSM Olympus FV1000 using excitation of the blue laser,  $\lambda=473$  nm, and making Z-Stacks of 4-7 shoots.

As the cases of unaligned IPL and PPL cell walls were obviously numerous, just a percentage of offset to aligned cells, a criterion successfully applied to *Timmia* (Budke *et al.*, 2007), may not represent the whole complexity. Thus a special procedure was developed to represent this complexity.

##### *Anatomy data performance*

Each photograph was reformatted in a geographic program to the “Mercator projection” (orthogonal projection of the Earth maps) using a basically geographic software ESRI ArcGIS 10.x (<http://www.esri.com>). The

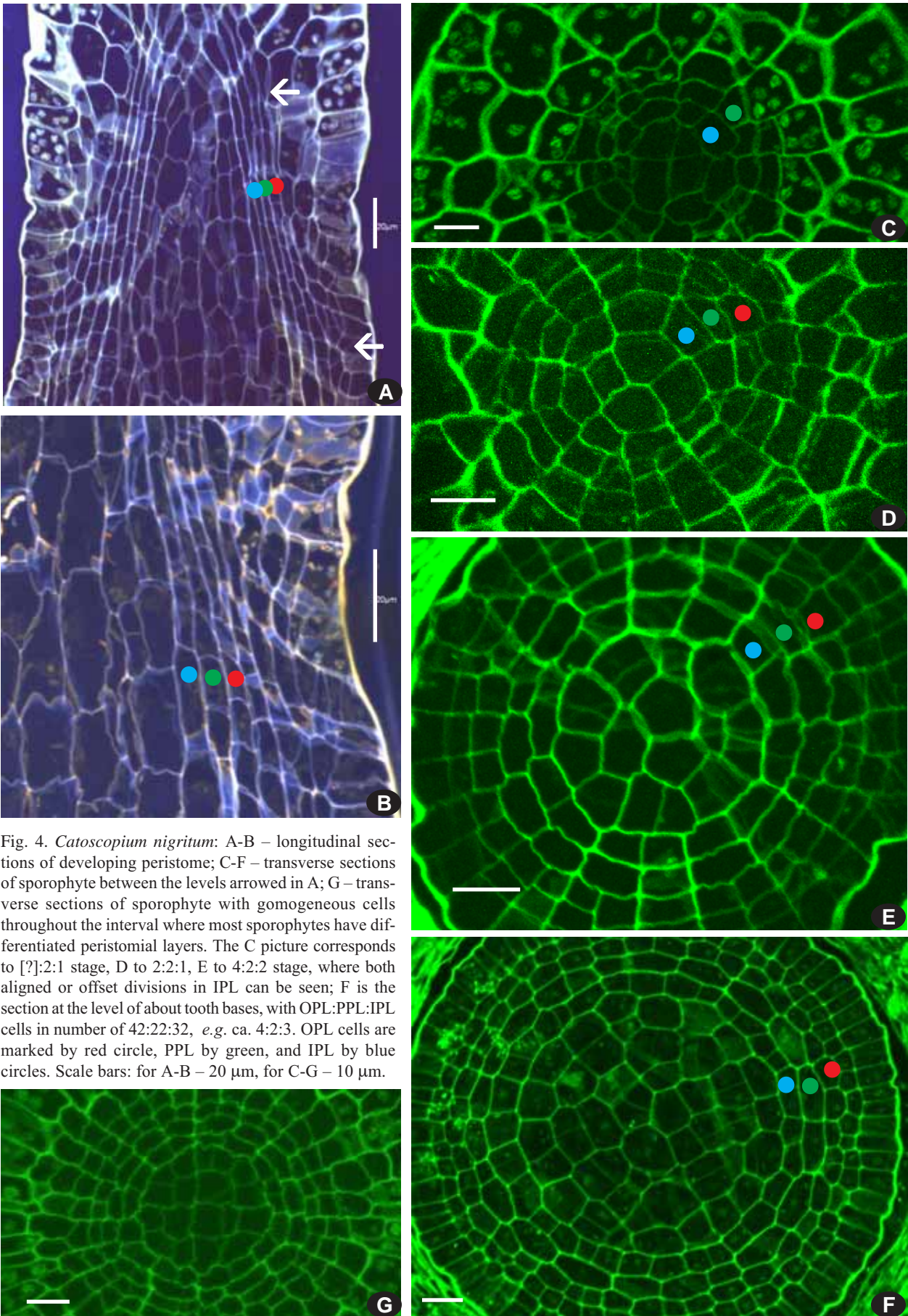


Fig. 4. *Catoscopium nigratum*: A-B – longitudinal sections of developing peristome; C-F – transverse sections of sporophyte between the levels arrowed in A; G – transverse sections of sporophyte with homogeneous cells throughout the interval where most sporophytes have differentiated peristomial layers. The C picture corresponds to [?]:2:1 stage, D to 2:2:1, E to 4:2:2 stage, where both aligned or offset divisions in IPL can be seen; F is the section at the level of about tooth bases, with OPL:PPL:IPL cells in number of 42:22:32, e.g. ca. 4:2:3. OPL cells are marked by red circle, PPL by green, and IPL by blue circles. Scale bars: for A-B – 20  $\mu$ m, for C-G – 10  $\mu$ m.

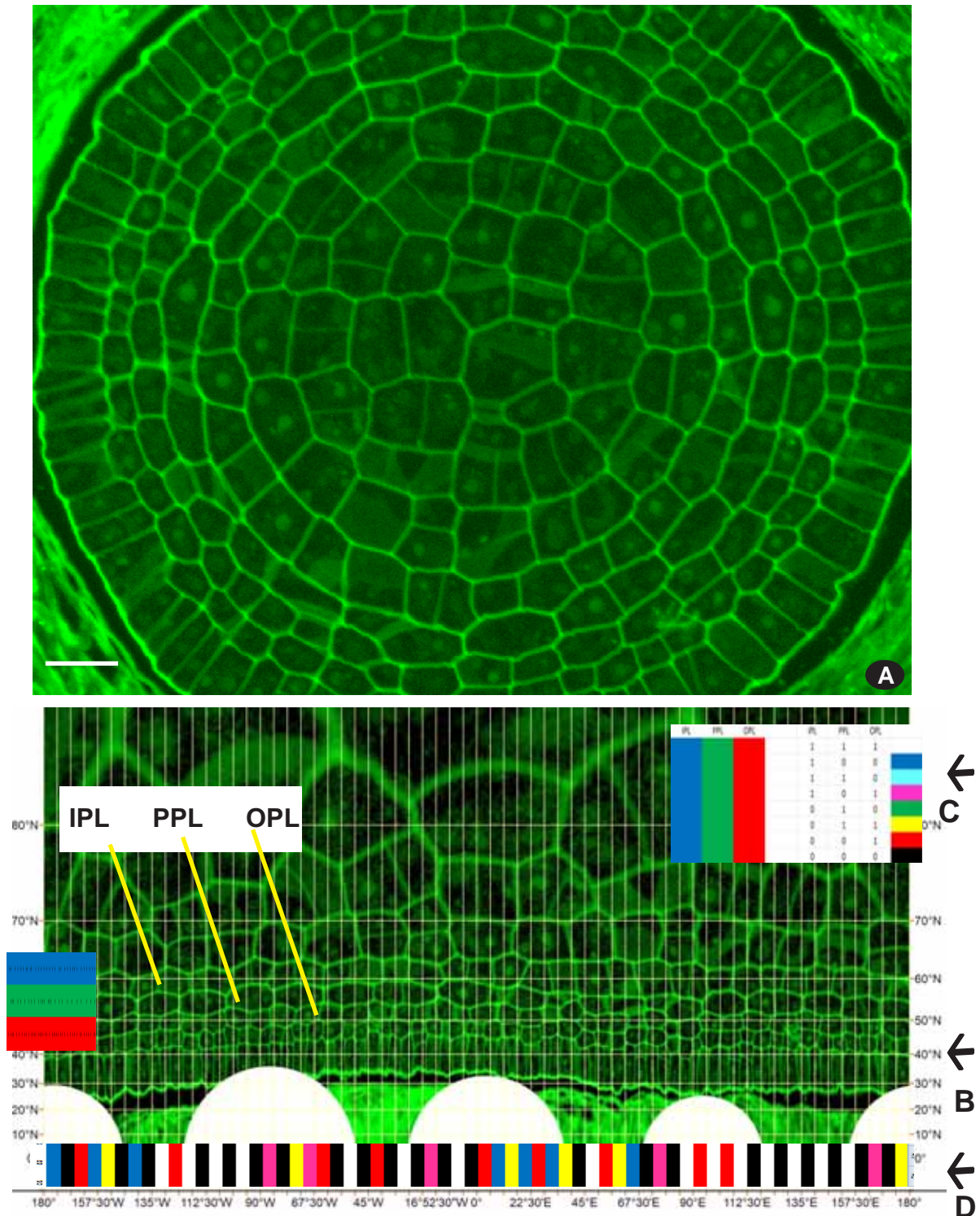


Fig. 5. Explanation of procedure of peristome structure RGB-coding: A – cross section, B – the same, transformed to “mercator” orthogonal projection; C – color coding of eight variants of peristomial layer cell walls presence or absence within 1/64 of the circumference; D – row of 64 color rectangles, corresponding to one transverse section. Scale bar: 10  $\mu$ m.

only modification was the change of 5° for minimal sector (default for Earth studies) to 5.75°, which subdivides the circular peristome image into 64 sectors (Fig. 5). As structural units in peristomes usually number 16 or 32 or, more rarely 64, we feel that such subdivision is detailed enough. Although 96 in some *Bryum* species and even 112

elements in *Roellia*, are known, these high numbers were ignored for the present study; however they may be easily added to the coding procedure if necessary.

A very important additional step during this transformation was to set zero, which allows aligning sections of the series with each other. Fortunately, well-vis-

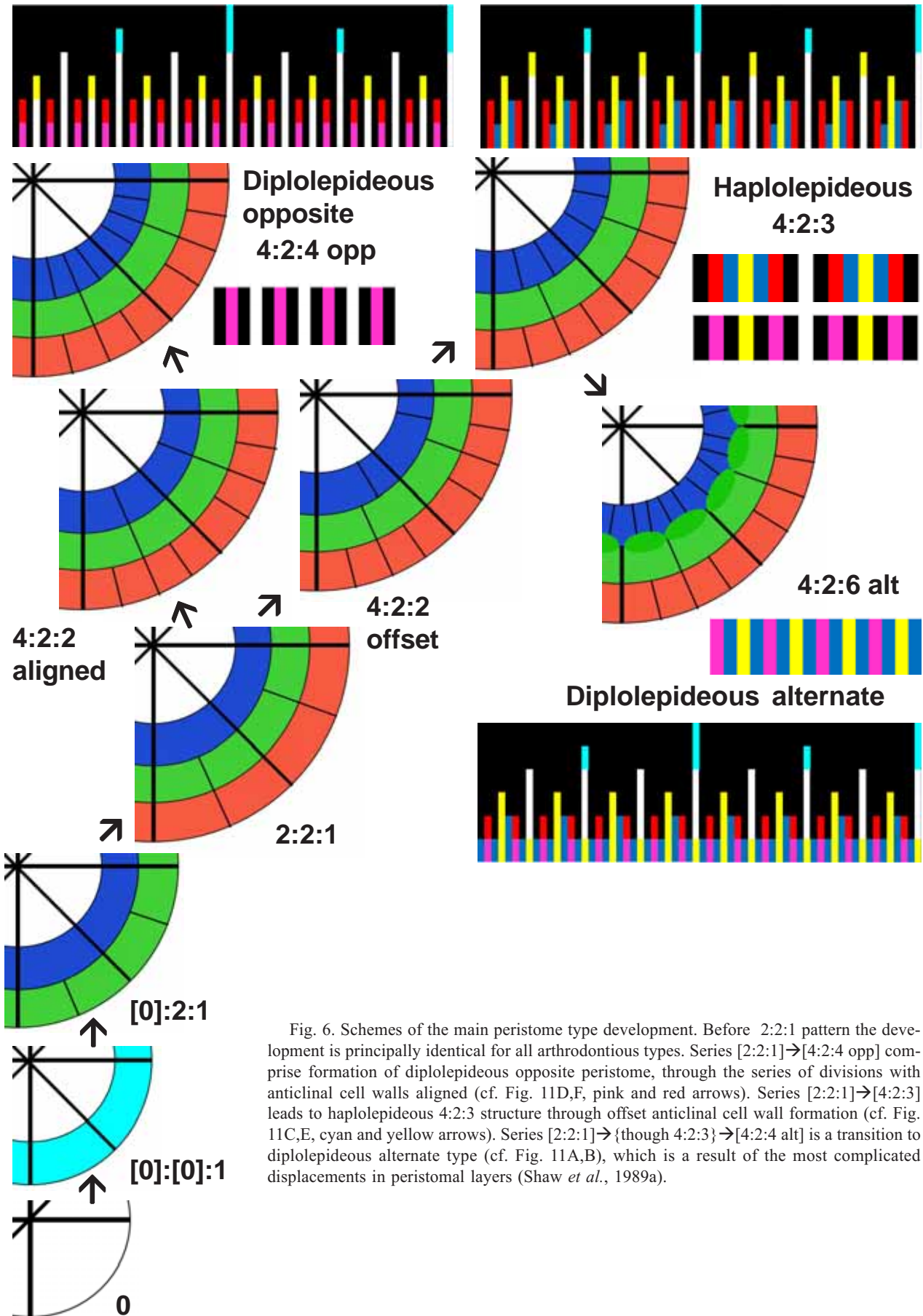


Fig. 6. Schemes of the main peristome type development. Before 2:2:1 pattern the development is principally identical for all arthrodoctious types. Series [2:2:1]→[4:2:4 opp] comprise formation of diplolepidous opposite peristome, through the series of divisions with anticlinal cell walls aligned (cf. Fig. 11D,F, pink and red arrows). Series [2:2:1]→[4:2:3] leads to haplolepidous 4:2:3 structure through offset anticlinal cell wall formation (cf. Fig. 11C,E, cyan and yellow arrows). Series [2:2:1]→{though 4:2:3}→[4:2:4 alt] is a transition to diplolepidous alternate type (cf. Fig. 11A,B), which is a result of the most complicated displacements in peristomal layers (Shaw *et al.*, 1989a).

ible crosses within the sporogene tissue (results of first three divisions in sporophyte), inside from the peristomial layers, help in most cases to accomplish this procedure without difficulty. The next moderately straightforward step was to check if each of 64 sectors in 3 layers had a cell wall or not. After this, one transverse section of capsule was transformed into 3×64 matrix, with states of + (present) or – (absent).

Attempts to use various 3D methods appeared to be too cumbersome. Coding in “RGB mode” (Fig. 5) provides a visual representation of the pattern in relation to the standard color patterns of the main types of peristome structure (Fig. 6).

We coded IPL as blue, PPL as green, and OPL as red. When one of 64 columns has a cell wall in only one layer, the color of this layer is a resulting one. When no cell wall occurs in the column, it is black, while if cell walls are in all three layers, the resulting color will be white, suggesting a complex nature of white light. Other combinations are also easy to interpret; for example, red+green=yellow, red+blue=pink (magenta), green+blue=cyan (Fig. 5).

In this way, one section is transformed into a band of 64 rectangles, each filled by one of 8 colors. The advantage of the method is that it allows an easy overview of many sections in a series with one figure, and provides an immediate impression of the peristome structure pattern not only at one level, but tracing it along all peristome teeth, checking if the structure is stable all along it or is changing, and in the latter case, to what extent and in what way.

Especially important for our purpose is the position of the white color, which indicates an aligned position in all three peristomial layers, as well as the yellow one, suggesting displacement, which is essential information for arthrodontous peristomes except for the basal group of four orders with diplolepidous-opposite peristomes: Gigasporales, Funariales s. l. (incl. Disceliales), Encalyptales, and Timmiales. Alternation of white, black and pink and total absence of yellow color is a characteristic of them. Contrary to that, the yellow-coded offset position of IPL against PPL+OPL indicates the structure of two main peristomial types: haplolepidous (Grimmiales, Dicranales, etc.) and diplolepidous-alternate (Bryales, Hypnales, etc.) peristomes.

Each of the main peristomial structures has a specific color pattern (Fig. 6), and the distribution of these patterns can be easily seen around the combined circumferences (Figs. 7-8). Note however that a slight difference in anticlinal cell wall position may change the color pattern (Fig. 6, haplolepidous; Fig. 7E-H). The ‘isomeric’ color patterns, however do not transfer from one type of the principal peristomial structure to another one.

Diplolepidous-alternate peristomes with numerous cilia, reflected by a formulae of 4:2:8-12(-14) may have very closely arranged anticlinal divisions, resulting in 2

and probably sometimes even 3 divisions within one of 1/64 sectors. This case almost never occurred in the present study of *Catoscopium*, although in diplolepidous-alternate peristomes it may happen and in this case may be marked by an asterisk for 2 and a double asterisk for 3 divisions in one layer within one sector.

After such RGB-coding by colors (Figs. 5), peristomes are ready to analyze. However, being applied to *Catoscopium*, which is likely a rather difficult and irregular case (Figs. 7-8), we had to be sure that it works in mosses with more regular peristome structure. For such a “control” we undertook a similar coding for *Podperaea krylovii* (Podp.) Z.Iwats. & Glime, a representative of Hypnales: Amblystegiaceae (Ignatov *et al.*, 2006, 2007) or Hypnaceae (Goffinet *et al.*, 2009), with a well developed or only slightly reduced peristome. Comparative to the fully developed diplolepidous-alternate peristome with 3-4(-6) cilia in the endostome (as in some species of *Bryum*), Hypnales display a somewhat less developed scenario, with most commonly 2 or more rarely 3 cilia, with common reductions to one or no cilia. The *Podperaea* endostome in most cases has one cilium (corresponding the formula 4:2:6), and more rarely two cilia or occasionally none between neighboring segments; three cilia were never observed in the studied collection of this species. Otherwise *Podperaea* comprises a case, which usually is described as a “hypnoid”, “perfect” or “fully developed” peristome (Fig. 9).

The protocol of preparation was essentially the same as for *Catoscopium*. Material used for this study was taken from the cultivation in MLR32 Sanyo, where the moss successfully grew about 9 months after being collected in September of 2013, in the Primorsky Territory of Russia (voucher Ignatov and Ignatova #13-1456, MHA).

#### *Editing for the better performance*

A disadvantage of this method is a sensitivity to noise because of the imperfect circles of peristomial layers that may also appear in the course of preparation, and such changes may lead to a modification of the color pattern. However this sensitivity is relative: wrong attribution of one anticlinal cell wall to a nearby 1/64 sector is easily visible and correctable, as a re-attribution of a cell wall to neighboring sector does not affect the overall peristomial formula. There are three variants for 4:4:4 (Figs. 7H, H', and H'') and three variants for 4:2:3 (Figs. 7E, E', and E''). For an easy understanding of the pattern in the subsequent scheme (cf. Fig. 7-8) the patterns 7E' and 7E'' were substituted by 7E. It is important in this case that the pattern 4:2:4, both diplolepidous-opposite and diplolepidous-alternate, comprise 4 color repeats, both unique for each of them (cf. Fig. 6), and only the haplolepidous 4:2:3 pattern has 8 color repeats in all three variants. And finally, 2 color repeats indicating a 4:4:4 pattern, should also be considered in the *Catoscopium* peristome, considering the opinion about its position in the Splachnales (Buck & Goffinet, 2000). *Splachnum* has a 4:4:4 pattern (Schwarz, 1994).

### Molecular phylogenetic analyses

Two different molecular data sets were compiled for the present study. 1) A concatenated data set of mitochondrial *nad5* and plastid *rps4* sequences for a small taxon subset consisting only of genera used for peristome development studies (Table 1), supplemented with few phylogenetically important genera, e.g. nomenclatural types of families and orders. Sequences were downloaded from Genbank, except for one newly generated *rps4* sequence for *Podperaea krylovii* (specimen: Russia, Altai, Ignatov #1/10, MHA, KT388714). 2) A slightly modified version of the bryophyte backbone data set by Wahrmond *et al.* (2010). In order to be more representative for the study group we included available sequence data for three *Diphyscium* species, instead of using a compound sequence for the genus. In addition, we included sequence data for *Scouleria aquatica* and *Bryoxiphium norvegicum*, but slightly reduced the out-group sampling, while complementing the data set with another plastid marker, the group I intron residing in *trnL* (*trnL* G1) which was readily available in GenBank (Appendices 1-2).

Alignment of the sequence data for both data sets was guided by the already established bryophyte backbone data set from Wahrmond *et al.* (2010). The taxonomic adjustments required only few alignment changes mainly in order to accommodate the microstructural evolution of group I intron residing in *nad5* (nad5i753). Similarly, for the appended *trnL* G1 the published structurally guided alignment of the intron for bryophytes was used as scaffold (Quandt & Stech, 2005). Based on the criteria laid out in Kelchner (2000) required modifications of the alignments were manually performed in PhyDE® v0.995 (www.phyde.de). Hotspot definitions followed Wahrmond *et al.* (2010) for both data sets. As *trnL* G1 was not included in Wahrmond *et al.* (2010) ambiguous parts of the alignment were defined to five hotspots following the strategy in Olsson *et al.* (2009). Detected inversions were positionally separated in the alignment and included as reverse complemented in the phylogenetic analyses, compare Quandt *et al.* (2003) and Borsch & Quandt (2009).

Maximum Likelihood (ML) reconstructions were done using RAxML (Stamatakis, 2014), applying the GTRGAMMA model for nucleotide evolution and F81 for indels. Internal branch support was estimated by heuristic bootstrap (BS) searches with 10,000 replicates each. Bayesian analyses were performed with MrBayes v3.2.5 (Ronquist *et al.*, 2012), generally applying the GTR+ $\Gamma$ +I model. The a priori probabilities supplied were those specified in the default settings of the program. Four runs with four chains ( $10^6$  generations each) were run simultaneously, with the temperature of each heated chain set to 0.2. Chains were sampled every 1000 generations and the respective trees written to a tree file. The output files were examined in Tracer v1.6 (Rambaut *et al.*, 2014) in

order to evaluate the effective sampling size and to ensure that the chains reached stationarity within the first 25%, which were discarded prior calculations of the consensus tree and the posterior probability of clades. Consensus topologies and support values from the different methodological approaches were compiled and drawn using TreeGraph 2.4.0-456 beta (Stöver & Müller 2010).

### RESULTS

**Observations under light microscope and SEM** showed a rather similar peristome structure in different specimens of *Catoscopium* (Figs. 1-2). In all studied specimens the peristome was strongly fragile, so in many cases tooth parts remained on the sticky paper used for mounting capsules on stubs for SEM observations, or attached to the inner side of the operculum (Fig. 1E-F). Teeth along the mouth were often represented by just their basal parts, and capsules with maximally developed peristomes were found quite a few times.

Exostome teeth have a median line on their outer surface; this surface is irregularly reticulate and papillose over most of the outer cell wall plates, except in a zone near the median line and plate margins, where the surface is perfectly smooth in some specimens. Sometimes the ornamentation reaches the tooth margin (Fig. 1H-K). A similar reticulate and papillose ornamentation also occurs on low faces outside the exostome, they are interpreted here as a preperistome of a very poor expression (Fig. 2A-D). It is formed by 1-3 rows of amphithecial cells outside of OPL (Fig. 2C-D).

The exostome teeth are 16, but sometimes 15 or 17 due to lateral fusion or division of some into small unequal entities, but these cases are rare and if teeth are more or less equally developed their number is 16 without exception. Teeth are irregular in shape, as plates are arranged not exactly one above another, making them variously curved and eroded (Fig. 1G-H). Dorsal trabeculae are absent, ventral ones are occasionally developed but are commonly very low (Figs. 1I-J, 2E-F). The inner surface of the exostome teeth is covered by large low papillae (Fig. 2G-H) or are smooth (Fig. 2F, I), and both types of surface ornamentation occur on the endostome inner surface as well (Fig. 2H-I), so it is not always apparent which surface is under observation. The adherent highly reduced endostome material is represented by a thin membrane at the tooth bases, only in few places separated by a distance less than one cell length (Fig. 2E, H-I), or otherwise the membrane may be firmly joined to the inner surface of a tooth, and in this case it can be recognized by the inner median line (Fig. 2E).

### Anatomy study

Peristomial layers were found in eight out of ten capsules cut transversely. They were apparent in (15-) 30 to 120 sections, 2  $\mu$ m thick, i.e. at (30-)60 to 240  $\mu$ m intervals. In two series amphithecium cells were quite homogeneous, as explained above (page 394), and were likely associated with ultimate reductions

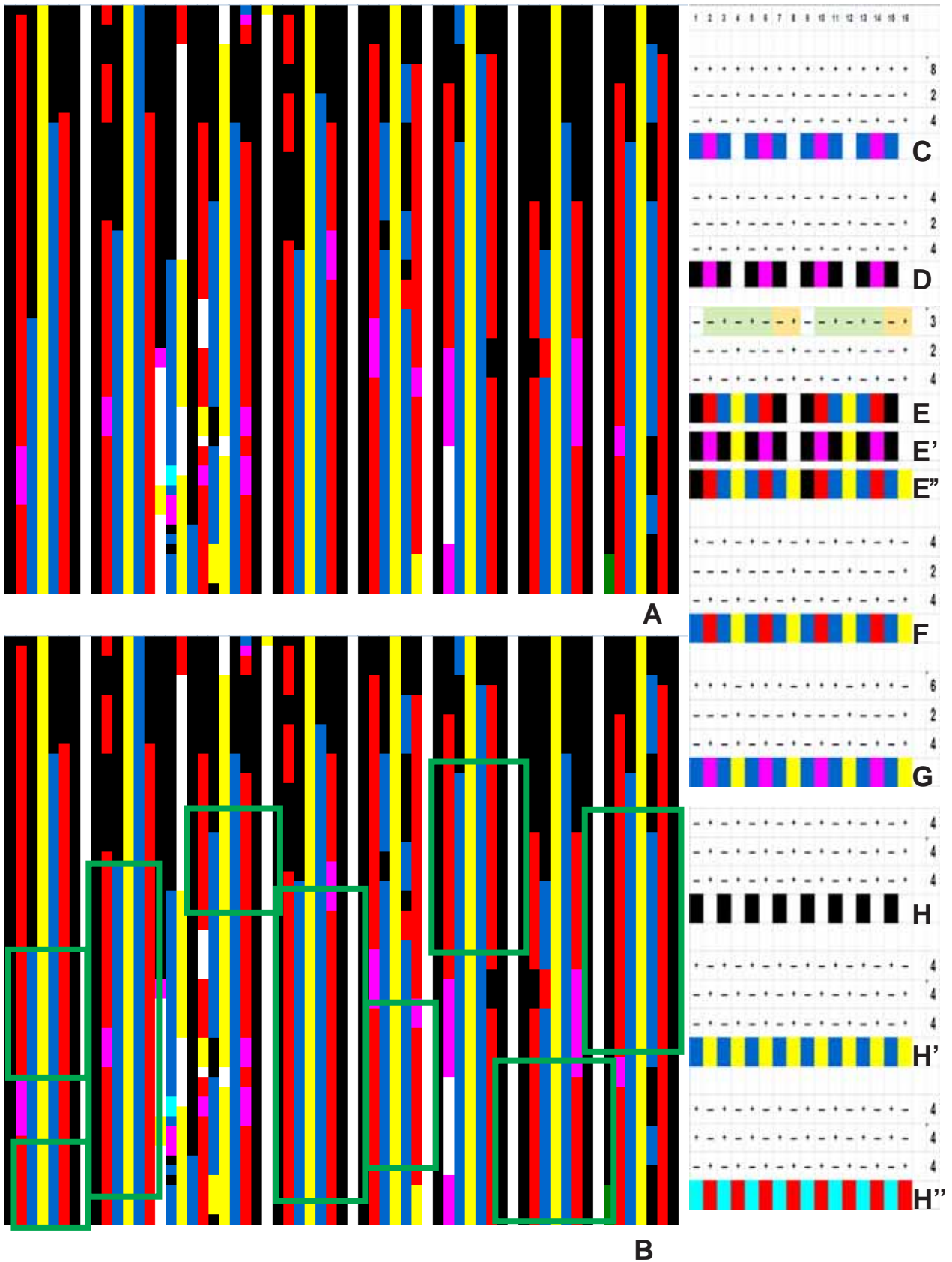


Fig. 7. *Catoscopium nigratum* peristome structure shown with RGB-coding, explained in Fig. 5. A-B – one capsule shown as the series of 60 RGB-coded cross sections, thus comprising 120  $\mu\text{m}$ . B is the same as A with green-boxed areas of typical 4:2:3 pattern of haplolepidous peristome structure; note that it occurs in many parts, although not throughout the peristome. C-H illustrate variants of color patterns characteristic to main peristome structures.

shown in Fig. 1C. They were not considered further in the present study.

Figs. 7 and 8 present two series of cross sections, coded by the RGB method, and Fig. 9 shows the reconstruction of the peristome of *Podperaea*, the 'control species'. Despite of a strongly variegated and somewhat irregular appearance of the *Catoscopium* series, the characteristic patterns (cf. Fig. 8) can be recognized, although not so apparent as in *Podperaea*.

Both series of *Catoscopium* (Figs. 7-8) comprise sporophytes at an early stage of development: additional divisions in PPL appear at the same level from the top, at about 100-120  $\mu\text{m}$  (compare with Fig. 4). Sporophytes at this level are 90  $\mu\text{m}$  in diameter, with endothecium 40  $\mu\text{m}$  in diameter. Nevertheless the appearance of the peristomial pattern is different, the capsule shown in Figs. 7 and 10A (cf. also Table 1A) has many more octants where 4:2:3 pattern is represented compared with Fig. 8 (see also Fig. 10C, Table 1G).

Distal parts of the developing peristome of *Catoscopium* mainly represent the alteration of aligned and offset cell divisions (coded as white and yellow correspondingly), *i.e.*, the stage of 2:2:1 (Fig. 4D), where earlier divisions of "fundamental cross", and one subsequent division in the PPL 8-celled circumference, which is a pattern almost universally present in all arthrodontous mosses (cf. Fig. 6). Additional amphithecial layers occur at the distal level of peristome (Fig. 4A), being 5-6(-7)-layered, and gradually reducing in number to the level of annulus, where amphithecium is usually 4-layered (cf. Fig. 4E-F).

The number of peristomial layers changes from 2 to 3 in the upper 10-20  $\mu\text{m}$ . (Hereafter distances are measured downwards to the level where peristomial layers become distinct). At this level, the PPL cells are already 16, a number which remains up to the middle or base of the teeth.

Anticlinal cell walls in IPL are formed at first only between the octants (Fig. 4C), being 8 in number (white lines in Figs. 7-8) in uppermost 10-20(-30)  $\mu\text{m}$  (rarely lower in some octants). At this point anticlinal divisions changing the formula from 2:2:1 to 4:4:2 appear. In RGB-coded schemes in Figs. 7-8 they appear as blue flanks along the yellow lines in the uppermost part of peristome. In all 8 sectors of all studied peristome series, the anticlinal cells walls in IPL originate (or, more precisely, become apparent through the present method) at approximately the same level among octants, and always at about 1 cell length distance within one octant. This appears as one blue flank of a yellow line differs from another blue flank to 10-20  $\mu\text{m}$ . This must be obligatory, as the division in the larger cells appears as a result at the stage of transition from 2:2:1 to 4:2:2 (Fig. 11A to 11B, and from 11C to 11D) and can not divide simultaneously to form 4:2:3 pattern.

This haplolepidous 4:2:3 pattern has been found in the distal parts in series of sections in *Catoscopium*, although the process in individual sporophytes may differ substantially (Fig. 10, Table 1).

Divisions in the OPL are 16 since the earlier stages of the series, appearing as white plus yellow lines in Figs. 7-8. Other divisions in OPL appear at the same level where the IPL divisions start, *i.e.* at 10-30  $\mu\text{m}$  from the peristome top or, more commonly, slightly above: note that "red lines" penetrate to the "level of white and yellow lines only", *i.e.* above the "blue lines of IPL divisions". Upper ends of "red lines" occur at about the same level.

Within the interval 20-30(-35)  $\mu\text{m}$  the arrangement of anticlinal cell divisions exhibits the haplolepidous, 4:2:3, pattern (Figs. 7 and 8). There are a number of exceptions due to either (1) lack of division in a cell where it would be expected due to the presence of anticlinal cell walls in the same column above and below this cell, or (2) an extra division, also appearing in just one cell or several cells one above another. Such exceptions are relatively few near at the level of transition of '8-celled IPL' to '16-celled IPL', *i.e.*, the place where the 4:2:3 pattern is maximally expressed.

The closer to teeth base of *Catoscopium*, the more numerous are exceptions from the 4:2:3 pattern, especially due to additional cell divisions in peristomial layers. The number of PPL cells exceeds 16 from about 70-80  $\mu\text{m}$  from the teeth tips (Figs. 7-8), increasing to 19-24 at the level of 200-240  $\mu\text{m}$ . However different series exhibit considerable variation in numbers of cells (Table 1).

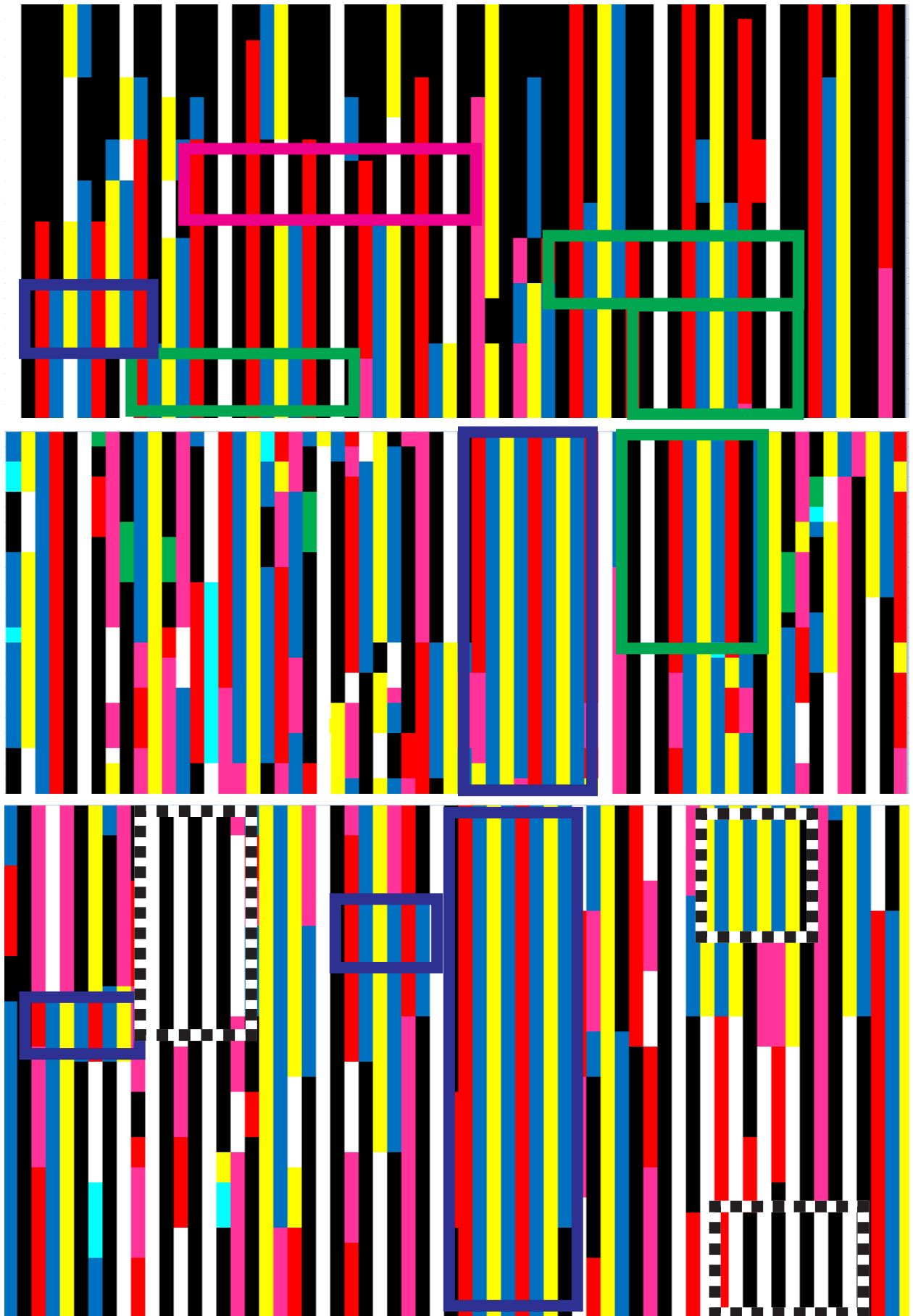
The 4:2:3 pattern either remains prevailing the individual series (Fig. 7, 10A, Table 1) or becomes rare (Fig. 10B) to totally disappearing (Fig. 8, 10C), being substituted by 4:2:4 alternate, 4:2:4 opposite and sometimes 4:4:4-patterns.

The diplolepidous-alternate pattern (cf. Fig. 6) appears occasionally in the upper third of the teeth (Fig. 7), but is more common in their proximal parts (Fig. 8).

The pattern 4:4:4 appears to be quite common in the proximal part of peristome, but at least partly this has to be referred as a methodological error: as the circumference has been divided into 64 segments, the additional divisions in PPL, even with stochastic positions of anticlinal cell walls, raise the probability for 4:4:4 pattern (see also discussion).

In the 'control species', *Podperaea*, two series were studied, one started from the 3-layered amphithecium (Fig. 9B), *i.e.*, since the 'pre-OPL stage'. The area 'transitional from 8 IPL to 16 IPL' (looking in the Fig. 9 as the level of 'upper ends of blue and red lines', cf. Fig. 7), occurs at 20-30  $\mu\text{m}$  from the top. It is principally the same as in *Catoscopium* (cf. Fig. 4D). Blue line ends are more uneven, often differing in the same octant at the 20-40(-80)  $\mu\text{m}$ .

The divisions in the IPL at the transition from 2:2:1 to 4:2:2 are mostly offset, thus the 4:2:2 pattern has un-



equal cells in IPL, the larger of them undergoes the next anticlinal division, making pattern 4:2:3 (Fig. 11A, yellow arrows). Further below one of IPL cells in each octant divides, resulting in a 4:2:4-alternate pattern (Fig. 11B, cyan arrows). This divided cell is usually the largest among other cells of a given octant, excluding the cell in octant center, *i.e.* that one forming subsequently the keel of the corresponding segment. The level where 4:2:4-alternate pattern prevails, *i.e.* corresponding to the structure with no cilia, were seen in both studied sections at the level ca. 30  $\mu\text{m}$  while further down towards the teeth base another cell other than the “keel progenitor” undergoes a division, approaching a 4:2:6 (Fig. 9F) and occasionally a 4:2:8 pattern.

At the level of 100  $\mu\text{m}$  a complete diplolepeidous-alternate pattern occurs almost throughout the capsule circumference. The main octants have 4:2:4 (red-blue-yellow-blue) or 4:2:6 (pink-blue-yellow-blue) pattern, except a few areas where the anticlinal cell walls in OPL, PPL and IPL are aligned throughout (shown in Fig. 9 as a white line).

Interestingly, in both *Podperaea* and *Catoscopium*, the anticlinal walls of the fundamental cross (in the distant part white and in ideal schemes cyan in color), mostly do not remain well aligned since the rather early stages, except one out of four rays of the “fundamental cross” which is more aligned than others (Figs. 4F, 10). So one (and most distinct) white line in *Podperaea* is a remnant of the first division.

#### Phylogenetic analyses

Phylogenetic analyses of both data sets provide a highly congruent picture (Fig. 12 & 13), with few conflicts, which are generally unsupported (*i.e.* posterior probabilities (PP) < 90 or bootstrap support (BS) < 80). The eperistomate groups are at the tree base (compare Wahrmond *et al.* (2010) for data set 2), followed by the nematodontous lineages, including *Tetraphis*. *Buxbaumia* receives a position between the nematodontous and the monophyletic arthodontous mosses (1.00 PP/100 BS). Among early diverging arthodontous mosses, *Diphyscium* represents the first branching lineage with maximal support. While the characteristic clades containing *i*) the diplolepeidous-opposite, *ii*) the haplolepeidous, and *iii*) the diplolepeidous-alternate mosses are each highly supported (PP > 0.99, BS > 90) the relationships among the three are controversial. Especially the position of *Timmia* is problematic, as with data set 2 it receives a sister group relation to the haplolepeidous and diplolepeidous-alternate mosses, whereas with data set 1 it is sister to a clade consisting of diplolepeidous-opposite and haplolepeidous mosses. However, in both cases support is not significant (*i.e.* PP < 0.95 and BS < 95). *Catoscopium* is continu-

ously resolved as first branching lineage among the haplolepeidous mosses, although in data set 2 *Timmia* joins *Catoscopium* in an unsupported clade sister to the rest of the haplolepeidous mosses.

#### DISCUSSION

Although an ideal method of peristome development study implies a complete series of earliest stages from the stage of four cells divided by “fundamental cross” after two first divisions (Fig. 5), it cannot be always applied to some rare species collected in remote areas, due to probable lack of some stages in specimens. However, as it is shown in series of capsule sections at later stages of development, these earlier stages are retained in a more or less intact state in distal parts of the capsule. At least the [0]:2:1 stage is clearly presented in both *Catoscopium* and *Podperaea* (Fig. 4C and 9B), once more confirming that the peristome has an outstandingly regular structure, due to synchronized divisions both in time and space (Shaw *et al.*, 1987; Shaw & Anderson, 1988).

As peristome development patterns prior the 2:2:1 stage are almost identical in both haplolepeidous and diplolepeidous mosses, including *Diphyscium* and even the nematodontous *Tetraphis* (cf. Figs. 12 & 13 for their phylogenetic positions), our study was concentrated on stages from the transition of 2:2:1 to 4:2:2, which were available in all studied series of cross sections, except those two that exhibited homogeneous cells throughout, without any apparently differentiated peristomial layers (Fig. 4G). Thus, eight series of transverse sections provide the basis for the following discussion of those stages of the peristome development, which are crucial for the peristome attribution to one of the types (Budke *et al.*, 2007; Shaw *et al.*, 2011).

The most common anticlinal divisions in the IPL at the transition of 2:2:1 to 4:4:2 are offset in *Catoscopium* (Table 1), thus the haplolepeidous pattern may be assumed as the “typical” or “basal” for this genus. This result agrees with the previously published molecular phylogenetic analyses (Quandt *et al.* 2007, Stech *et al.*, 2012; Inoue & Tsubota, 2014; Wahrmond *et al.*, 2010), as well as the analysis shown in Fig. 12 & 13. At the same time, this position of *Catoscopium* is close to the divergence point of mosses into the three main lineages: haplolepeidous, diplolepeidous-alternate and diplolepeidous-opposite groups (cf. Fig. 6) and *Timmia*.

Therefore the occurrence of the three basic patterns was the subject for a search within *Catoscopium*.

1. The haplolepeidous pattern (4:2:3) occurs at the level of the distal third of teeth in all series obtained, except those where amphithecial cells were homogeneous and peristomial layers were not recognized at all. At the level of transition from 2:2:1 to 4:2:2, the haplolepeidous

Fig. 8: Illustrations of the reduction patterns by three parts of peristome of *Catoscopium* in interval 10-60  $\mu\text{m}$ , then 100-130  $\mu\text{m}$  and 160-240  $\mu\text{m}$  from top. Upper part shows presence on 4:2:3 pattern (green boxes) and rarer 4:2:4 opposite pattern (purple box), while in the proximal part of peristome 4:2:4 alternate pattern (blue boxes) occurs among prevailing 4:4:4 pattern (hatched boxes).

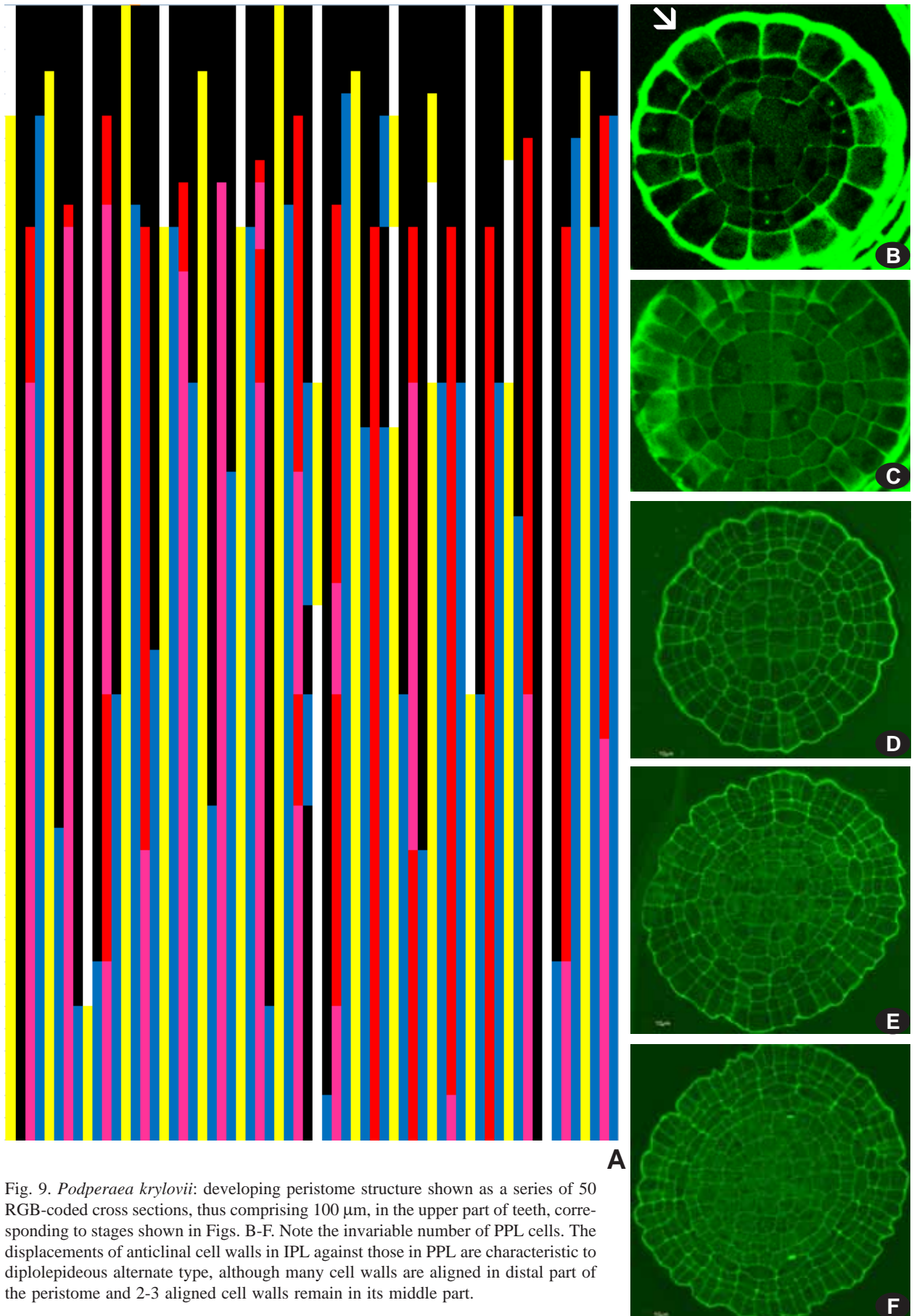


Fig. 9. *Podperaea krylovii*: developing peristome structure shown as a series of 50 RGB-coded cross sections, thus comprising 100  $\mu\text{m}$ , in the upper part of teeth, corresponding to stages shown in Figs. B-F. Note the invariable number of PPL cells. The displacements of anticlinal cell walls in IPL against those in PPL are characteristic to diplolepidous alternate type, although many cell walls are aligned in distal part of the peristome and 2-3 aligned cell walls remain in its middle part.

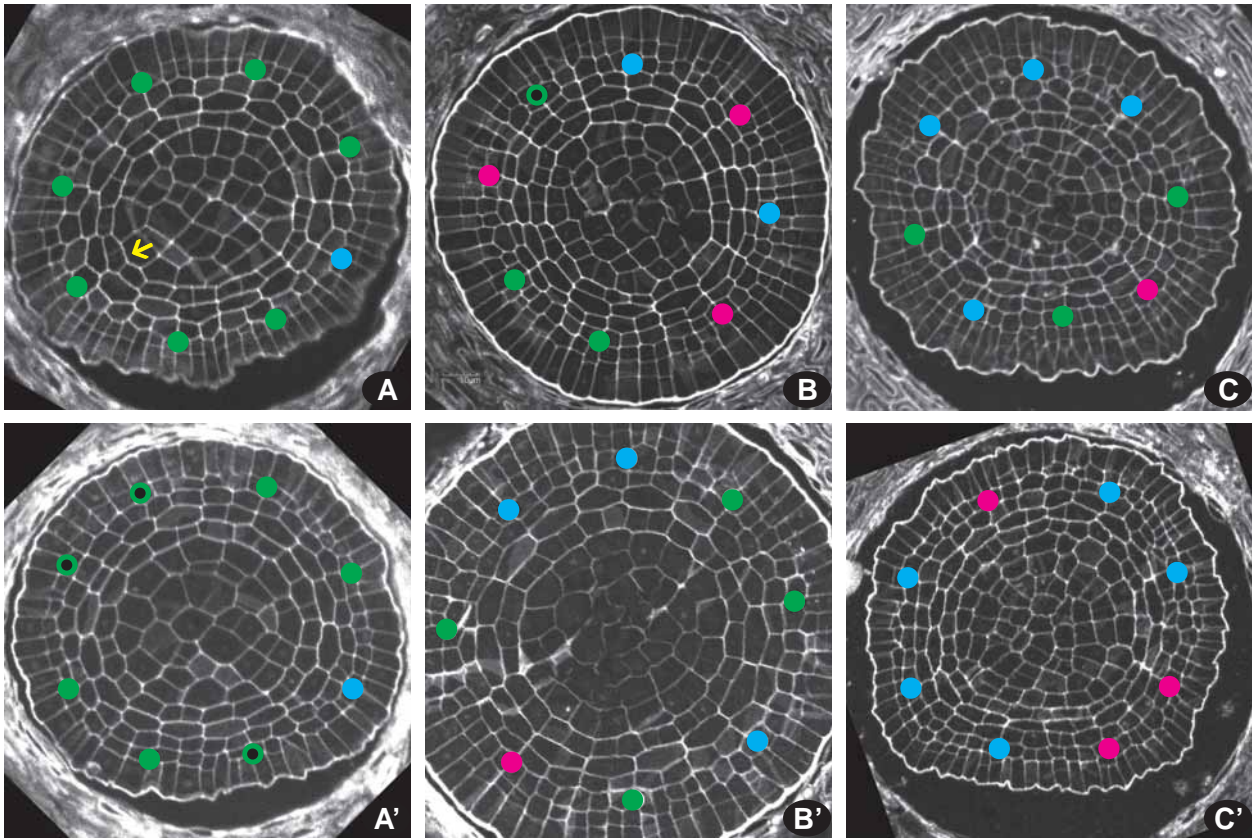


Fig. 10. A, B, C: selected sections from series of three *Catoscopium* developing sporophytes (cf. Table 1), at distance ca 50  $\mu\text{m}$  between A and A', etc.). For each octants the peristomial formula is evaluated and marked in green for 4:2:3; blue for 4:2:4 alternate and purple for 4:2:4 opposite. Black dot in the color circle indicates approximate evaluation.

color pattern is maximally expressed (Figs. 7-8), although in different series the 4:2:3 pattern is not equally clear. Comparison of the series shown in Figs. 7 and 8 demonstrates that in the former this 4:2:3 pattern is expressed in more places than in the latter (cf. also Fig. 10A,C and Table 1). Other examples of poorly expressed haplolepidous pattern are shown in Fig. 4E, 10B.

Note that the 'haplolepidous' lineages of moss evolution, represented by Dicranales s.l. (incl. Pottiales), Grimmiales, Bryoxiphales, Scouleriales, are characterized by the haplolepidous peristome structure, 0:2:3 in general, but in some rare cases short exostome teeth are formed and then peristome formula is 4:2:3, with the exostome having a median line, *i.e.* being thus diplolepidous. One case of this kind is described by Edwards (1979), for *Hypodontium*. Thus the 'haplolepidous lineage' may include groups with diplolepidous peristomes, albeit this is a rare case. In ca. 99% of species of 'haplolepidous lineage', in the course of maturation, the haplolepidous peristomes are reduced to a 0:2:3 pattern, with implies the total loss of the exostome.

In the proximal part of peristome (Figs. 7-8) the 4:2:3 pattern is obscured by additional divisions in all the peristomial layers and due to partial displacements of IPL cells to positions offset relative to PPL anticlinal cell walls (Fig. 10C). Interestingly, the total cell number in three

peristomial layers keeps the 4:2:3 proportion: in eight series proximal sections have: 35:18:24, 42:21:28, *etc.* Additional divisions were found to be common in Ditrichaceae by Shaw *et al.* (1989b), resulting in a formula of 4:2:4-6. Approaching formally to the diplolepidous-alternate formula, *Ditrichum* and *Dicranum* are characterized by no or very slight displacement of anticlinal cell walls between octants, which borders are markedly aligned with anticlinal cell walls of all three peristomial layers. Four out of eight such patterns continue into rays of the fundamental cross, still recognizable in endothecium.

2. The diplolepidous-opposite pattern (4:2:4) at the level of the distal part of the developing peristome appears "as a mirror" from the previous, 4:2:3 one: if a division is not distinctly offset, it is either perfectly aligned or subaligned (slightly offset), but the latter still leads to the scenario as it would be if they were perfectly aligned (cf. example in Fig. 11D, F). In the distal third of the peristome of *Catoscopium* the 'aligned pattern' appears in various places, where the first division in the IPL has happened not "enough unequal" to preclude the subsequent division in the smaller daughter cell. Usually aligned and subaligned patterns occur in 1-2, rarely in 3-4 octants (Fig. 4, 7-8, 10). The exceptionally homogeneous pattern, mentioned as presented in two series, leads

A(f)									E (l)							
1:1:1	2:2:2	2:1:1	2:2:1	2:2:1	2:2:1	2:2:1	2:2:1	2:2:1	4:2:2a	4:2:2a	3:2:2o	4:2:2o	4:2:2o	3:2:2o	4:2:2o	2:2:2a
1:1:1	4:2:1	2:1:1	2:2:1	2:2:1	2:2:1	2:2:1	2:2:1	2:2:1	4:2:2o	4:2:2o	3:2:2o	4:2:2o	4:2:2o	4:2:2o	4:2:3	4:2:2o
3:2:2	2:2:1	3:2:2	3:2:1	4:2:2	2:2:1	3:2:2	4:2:2		4:2:2o	4:2:3	4:2:2o	4:2:2o	4:2:2o	4:2:2o	4:2:3	4:2:2o
3:2:2	4:2:2	3:2:2	4:2:2	4:2:2	2:2:2	4:2:3	4:2:2		4:2:3	4:2:2	3:2:2	6:4:2	4:2:2	3:2:2	3:2:2	4:2:2
3:2:2	4:2:3	3:2:2	4:2:2	4:2:3	4:2:2	4:2:3	4:2:2		4:2:3	5:3:2	3:2:2	6:3:4	4:2:4a	4:2:3a	4:2:3o	4:2:2
[4:2:3]	[4:2:3]	4:2:3	4:2:2	4:2:3	4:2:3	4:2:3	4:2:4	4:2:2	F (a)							
4:2:3	4:2:3	4:2:2	4:2:3	4:2:3	4:2:3	4:2:3	4:2:3	4:2:3	2:2:1	2:2:1	2:2:1	2:2:1	2:2:1	2:2:1	2:2:1	2:2:1
4:2:3	4:2:4	4:2:3	4:2:3	4:2:2	5:2:4	3:2:4	4:2:3		3:2:1	4:2:1	2:2:1	4:2:1	3:2:2	3:2:2	4:2:1	3:2:1
4:2:3	4:2:4	4:2:3	4:2:3	4:2:2	4:2:4	3:2:4	4:2:3		4:2:2	4:2:3	4:2:2	3:2:1	4:2:4	[4:2:1]	3:2:1	4:2:2
4:2:3	5:3:4	4:2:3	4:2:3	4:2:2	4:2:2	4:2:3	4:2:3		4:2:2	4:3:3	4:2:2	3:2:1	5:2:3	[4:2:2]	4:2:2	4:2:2
4:2:3	5:3:4	4:2:2	4:2:3	4:2:2	3:2:2	4:2:4	4:3:3		4:2:2	4:2:2	4:2:3	3:2:3	4:2:3	4:2:2	4:2:2	3:2:3
4:2:3	6:3:4	4:2:2	5:3:3	4:3:3	4:3:3	4:2:3	4:3:4		-	-	-	-	-	-	-	-
5:3:4	4:3:3	4:2:3	4:2:2	3:2:2	4:2:3	4:2:3	4:2:3		4:2:4	4:2:2	4:2:3	3:2:3	5:2:3	4:3:2	4:2:2	4:2:3
6:3:4	4:2:3	4:3:3	5:2:2	4:3:3	4:2:3	4:2:3	4:2:3		4:2:4	4:2:4	4:2:3	4:2:2	4:2:3	4:2:2	4:2:4	4:2:3
B (i)									G(h)							
3:2:1	4:2:1	4:2:1	3:2:1	4:2:1	3:2:1	3:2:2	4:2:1		3:2:1	2:2:1	4:2:1	2:2:1	2:2:1	2:2:1	2:2:1	2:2:1
3:2:1	4:2:1	4:2:1	4:2:1	4:2:1	3:2:1	4:2:2	3:2:1		4:2:2o	4:2:1	4:2:1	2:2:1	4:2:1	2:2:1	4:2:2a	2:2:1
4:2:2	4:2:3	4:2:2	4:2:2	4:2:2	4:2:3	4:2:2	2:2:1		4:2:2o	3:2:2o	2:2:3	4:2:2o	4:2:2a	3:2:2a	3:2:1	2:2:1
4:2:2	4:2:2	4:2:2	4:2:3	4:3:3	4:2:2	5:3:3	4:2:2		4:2:3	3:2:2a	2:2:3	2:2:2a	4:2:2a	4:2:2a	3:2:2a	2:2:2a
5:2:2	4:2:2	4:2:2	4:2:4	4:3:3	4:2:2	5:2:2	3:2:4		4:2:3	3:2:3	4:2:3	4:2:3	4:2:3	4:2:2o	4:2:3	4:2:2a
4:2:3	4:2:4	4:2:4	4:2:4	4:3:3	4:2:3	4:2:4	4:2:2		4:2:4	2:2:3	4:2:4	4:2:3	4:2:3	4:2:3	4:2:3	4:2:2a
4:2:4	4:2:4	4:2:4	4:2:4	4:2:4	4:2:3	4:2:4	4:2:3		4:2:4	4:2:3	4:2:4	5:2:4	4:2:3	4:2:3	3:2:3	3:2:3
4:2:4	4:2:3	4:2:4	4:2:4	4:2:4	4:2:3	4:2:4	4:2:3		4:2:4	4:2:3	4:3:4	4:3:4	5:3:3	4:2:3	3:2:4	4:2:3
4:2:4	4:2:3	4:2:4	4:2:4	4:2:4	4:2:3	4:3:3	4:2:4		4:3:4	4:2:4	4:3:4	5:4:4	4:2:4	6:2:3	4:2:4	5:3:3
4:2:4	4:2:3	4:2:4	4:2:3	5:2:3	6:3:6	5:3:4	4:3:3		4:3:4	4:2:4	4:2:4	5:4:4	4:3:4	5:2:2	4:2:4	5:3:4
C (b)									6:3:4	6:2:4	6:2:4	4:3:4	4:3:4	4:2:3	4:2:4	5:3:3
2:2:1	4:2:3	3:2:1	2:2:1	2:2:1	2:2:2a	3:2:1	3:2:1		5:3:4	4:3:4	4:2:3	4:3:4	5:3:4	5:2:3	4:2:4	6:3:3
2:2:1	4:2:3	3:2:1	2:2:1	4:2:2o	2:2:2a	3:2:2o	3:2:2o		4:3:4	4:3:4	6:3:3	5:3:4	5:4:4	4:2:3	4:2:4	6:2:3
D (d)									5:3:4	6:3:4	6:2:3	6:3:4	4:4:4	4:2:4	4:2:4	6:3:3
0:1	0:1	0:1	0:1	0:1	0:1	0:1	0:1	1	7:4:4	6:2:4	5:3:5	4:2:3	4:4:4	4:3:4	5:2:4	4:2:4
2:2:1	2:2:1	2:2:1	2:2:1	2:2:1	2:2:1	2:2:1	2:2:1	42	8:4:4	7:2:4	4:2:3	4:2:2	5:4:4	4:2:4	5:2:4	4:2:3
4:2:2	4:2:2	4:2:2	4:2:2	4:2:2	4:2:2	4:2:2	4:2:2	108	6:4:4	7:4:4	5:5:3	4:4:4	5:3:4	4:2:3	4:2:3	4:3:4
4:2:2	4:2:3	4:2:2	4:2:2	4:2:2	4:2:3	4:2:3	4:2:3	126	6:4:4	8:4:4	4:4:4	4:3:3	5:2:3	4:2:3	4:3:3	4:3:4
4:2:2	4:2:3	4:2:2	4:2:2	4:2:2	4:2:3	4:2:3	4:2:3	150	6:4:4	7:4:3	4:3:4	6:2:3	5:2:3	4:2:3	4:2:3	5:4:4
4:2:3	4:2:3	4:2:4	4:2:4	4:2:2	4:2:3	4:2:3	4:2:3	164	4:2:3	6:4:3	6:4:3	4:2:4	6:3:4	4:3:3	4:3:4	4:2:3
4:2:3	4:2:3	4:2:4	4:2:4	4:2:2	4:2:3	4:2:3	4:2:3	188	Table 1. Peristomial formulae for each of eighth octants of the studied sporophytes of <i>Catoscopium</i> . Formulae are shown with distance 10 µm one from another, if otherwise is not specified [number at the right margin in D series].							
4:2:3	4:2:3	4:2:4	4:2:2	4:2:3	4:2:3	4:2:3	4:2:3	218								

to a strong peristomial reduction, likely similar to the example shown in Fig. 4G. Almost all anticlinal divisions are aligned in those cases.

In the proximal parts of the peristome, the color-pattern corresponding to 4:4:4 (cf. Fig. 5) appears to be sporadic in 4 octants (Fig. 8). This pattern however can be a result of at least two developmental pathways: (1) either it is a continuation of 4:2:4-opposite pattern by additional divisions in PPL (like *e.g.* in *Splachnum*, cf. Schwartz, 1994), or (2) develops from 4:2:3 in those parts of circumference where cells underwent additional divisions, being one of restrictions derived from the RGB performance method, with the peristome subdivision into 64 sectors. Having not a full resolution of the sequence of cell divisions, the 4:4:4 areas in Fig. 8 reveal an interesting aspect, showing that the 4:4:4 patterns are expressed in opposite sides of the capsule, being determined likely by the urn curvature. Note that

additional divisions in PPL make the current method unable to differentiate the principal structure of 4:4:4 based on aligned anticlinal cell walls and pattern formed due to additional divisions. This question has to be addressed specifically in each case where problems with its interpretation appear. In *Catoscopium* the 4:4:4 pattern is represented in Fig. 8 in hatched frames; however, a close up view demonstrates its variable nature, not similar to that of *e.g.* *Splachnum*.

3. The diplolepidious-alternate patterns appear in *Catoscopium* peristomes closer to the base (Figs. 8, 10). Their occurrence is partly affected by irregular displacements, thus it might be assumed as a noise that is caused by an inappropriateness of the method; however, at places it has much in common with the pattern observed in *Bryum* (Shaw, 1989a). Fig. 4F shows the early displacement of the IPL cells relative to anticlinal cell walls in PPL, including those four formed at the beginning of

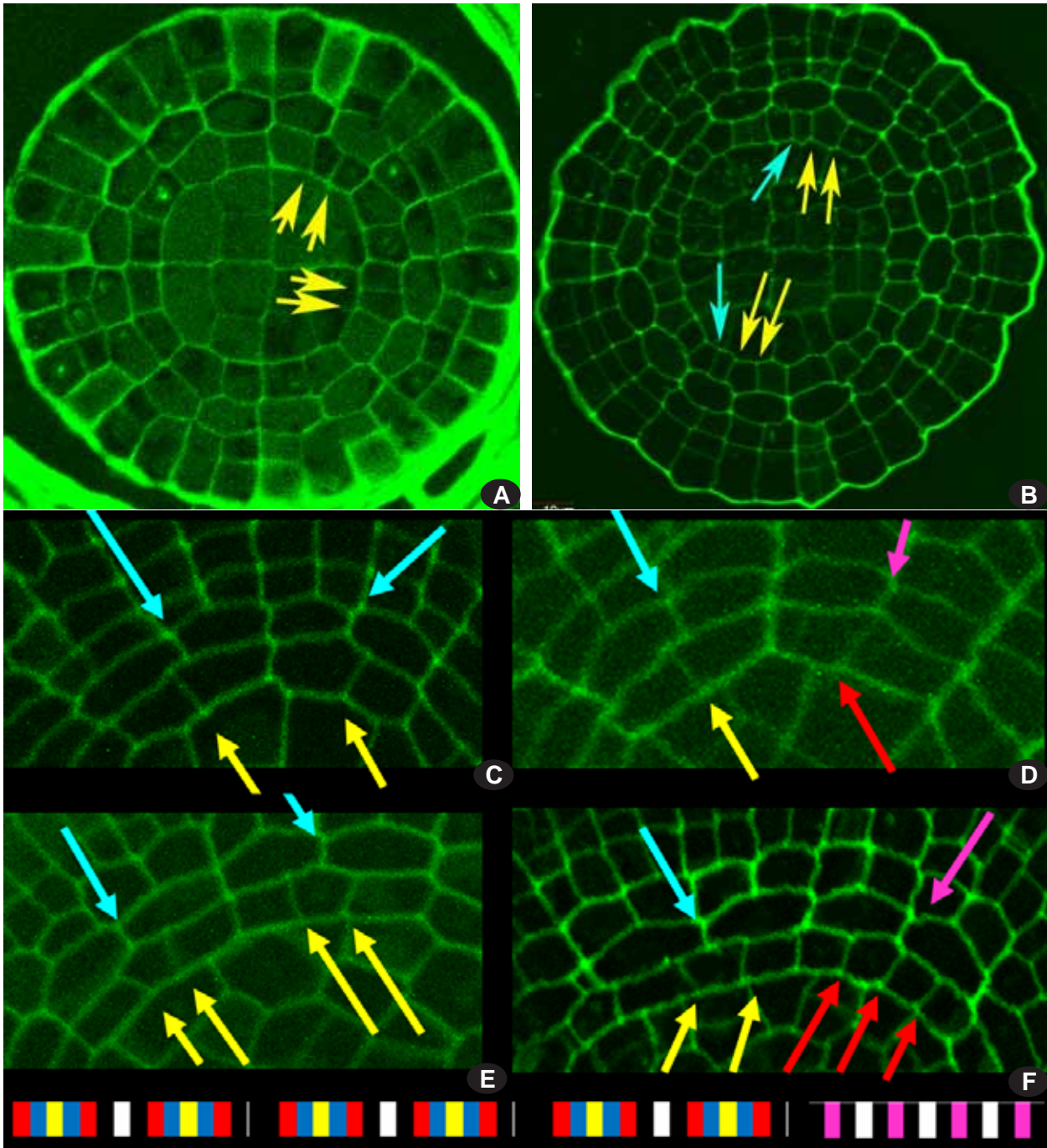


Fig. 11. A-B, *Podperaea krylovii*, sections (20 and 50  $\mu\text{m}$  from the upper point where peristomial layers become discernible), showing development of 4:2:4 (diplolepeideous-alternate) pattern through the stage of 4:2:3. C-F, *Catoscopium nigratum*, selected parts of sections, showing typical transition from 4:2:2 offset (C) to 4:2:3 (E), and less common transition from 4:2:2 aligned (D) to 4:2:4 aligned (F).

sporophyte formation and forming its ‘basic cross’, of aligned quadrant at the earlier stages. In all cases where it has been studied, including *Aulacomnium heterostichum* (Blomquist & Robertson, 1941), *Bryum bicolor* (Shaw *et al.*, 1989a), and *Podperaea krylovii* (Fig. 10), the early stages of development are characterized by the numerous divisions in IPL, so its cells become much smaller than cells in PPL, and these active divisions and local growth are associated with displacements, which do not occur usually in diplolepeideous-opposite

and haplolepeideous peristomes. However, contrary to the diplolepeideous-alternate mosses, in *Catoscopium* additional divisions involve not only IPL, but also PPL (resulting, as it was noted above, in retaining the overall 4:2:3 formula, as in the ‘classical’ variant, the 32:16:24).

Summing up, the haplolepeideous peristomial formula, 4:2:3, should be accepted as basic for *Catoscopium* due to prevailing offset divisions at the transition from 2:2:1 to 4:2:2 in most studied capsules, and presence of

some cross section series almost totally composed of octants with 4:2:3, including one where a complete series of developmental stages is present, starting from the two-cell-layered amphithecium. However, deviations are numerous, and as it makes the structure less regular, it can be called a reduction, as commonly used in bryological literature.

**Reduction of *Catoscopium* peristome** involves at least two trends: additional divisions in all peristomial layers and aligned instead of offset divisions at the stage changing formula from 2:2:1 to 4:2:2.

Additional divisions in the IPL were found also in *Ditrichum* (Shaw *et al.*, 1989b) and *Glyphomitrium* (Estébanez *et al.*, 2006), showing a certain parallel with the diplolepeidous-alternate pattern. An increase in PPL cell number is known in some diplolepeidous-alternate groups, *e.g.*, it is well known in *Bryum angustirete* and *B. arcticum* and correlates with (and is likely caused by) an adjoining of exo- and endostome. The fused structure may be considered as a reduction as it is associated with the loss of cilia, reducing hygroscopic ability which is well performed in *Bryum* species with complete, or perfect, peristomes.

**A trend from unequal divisions in the IPL to equal ones** occurs occasionally in some octants in developing peristomes of *Catoscopium* (Figs. 10, 11C-F). It seems that parallel changes occur in *Ephemerium*, *Tetraplodon* and *Splachnum* (Schwartz, 1994) and *Dichelodontium* (Magill, 1987): according to the molecular phylogenies these taxa do not belong to groups with diplolepeidous-opposite peristomes, but such peristomes are, however, present in these genera. In all cases this is correlated with overall sporophyte reduction (*Ephemerium*), or with considerable reduction of hygroscopic peristomial movements, especially strongly modified in *Splachnum* and *Tetraplodon* due to their unusual spore release by a slow pushing off by a specific false columella (Demidova & Filin, 1994).

Coming back to questions asked in the beginning of the study, “is it possible to recognize the basic peristome formula in irregularly developed peristomes of *Catoscopium*?”, the answer appears to be more complicated than just yes or no. It comes out that the 4:2:3 formula occurs at the earlier stages of development in *Catoscopium*, but this pattern is not 100% specific for haplolepeidous mosses. Diplolepeidous-alternate peristomes pass through the stage of 4:2:3 (Fig. 11A-B), and, probably even more important is the presence of this pattern in *Disphyscium* (Shaw *et al.*, 1987). Shaw *et al.* (1989b) challenged the idea that this stage is characteristic for the diplolepeidous-alternate mosses, as has been noted for *Aulacomnium* by Blomquist & Robertson (1941). According to the former authors this is no more than a very short transitional stage in the early development, as they found for the *Bryum* species (Shaw *et al.*, 1988). Although this principally agrees with what

we found in *Podperaea*, the 4:2:3 stage in *Podperaea* is more or less invariably formed and gradually transits to the 4:2:4-alternate pattern (Fig. 11). The explanation for this difference may depend on the slightly less developed peristome in *Podperaea* compared to *Bryum*: the former has (0-)1(-2) cilia, instead of usually 2-4 in *Bryum*. In *Podperaea*, subsequent divisions result in shifting of anticlinal cell walls in between octants to the offset position, a characteristic of diplolepeidous-alternate mosses. In *Catoscopium* the 4:2:4-alternate pattern is also not rare, especially close to the middle and basal parts of teeth, although occasionally appearing in the distal part or developing peristome as well (Fig. 10).

Subsequent swelling of PPL cells is considered to be the most important advanced character of diplolepeidous-alternate peristome (Shaw *et al.*, 1989b), differentiating it from the haplolepeidous mosses with additional divisions in IPL. Middle stages of development might look more or less similar in *Catoscopium* and *Podperaea* (cf. Figs. 4 and 9), although further towards the peristome base, the swelling is more conspicuous, and more additional anticlinal divisions occur in the IPL.

This overall differentiation of basic peristome types poses a question of their classification: what is the crucial for that? Either later stages, as argued Shaw *et al.* (1989b), or the youngest one, at a level of transition from 2:2:1 to 4:2:2, suggested as the most important in the peristome analysis of the genus *Timmia* (Budke *et al.*, 2007) where later stages comprise swelling (Murphy, 1988), obscuring the originally aligned cell arrangement.

Of course, it can be concluded that divergence in peristome development between the diplolepeidous-opposite type (including *Funaria*-type, *Timmia*-type, *etc.*) and all other types happens earlier, when 2:2:1 develops to 4:2:2, where IPL division can be either offset or aligned, whereas the divergence between haplolepeidous and diplolepeidous-alternate types becomes apparent at a slightly later stage of peristome development. This scenario nicely corresponds with the majority of phylogenetic trees (*e.g.* Newton *et al.*, 2000; Cox *et al.*, 2010). However the case of *Diphyscium* makes the situation more complicated: being basal in arthroodontous mosses, it has a very clear 4:2:3 stage, although later it is modified to strongly swelling pattern.

Taking into account the aforementioned observations, including the distribution of peristomial structures along the moss phylogeny (Figs. 12 & 13), the subordinate position of the 4:2:3-pattern as being characteristic for haplolepeidous mosses can be challenged. The further parallel was drawn by Shaw *et al.* (1987) with *Tetraphis*, which also has an offset divisions rather than aligned ones at the transition from 2:2:1 to 4:2:2 (although later its developmental pattern changes). Accepting this point, the 4:2:4 opposite pattern can be reconsidered as a re-

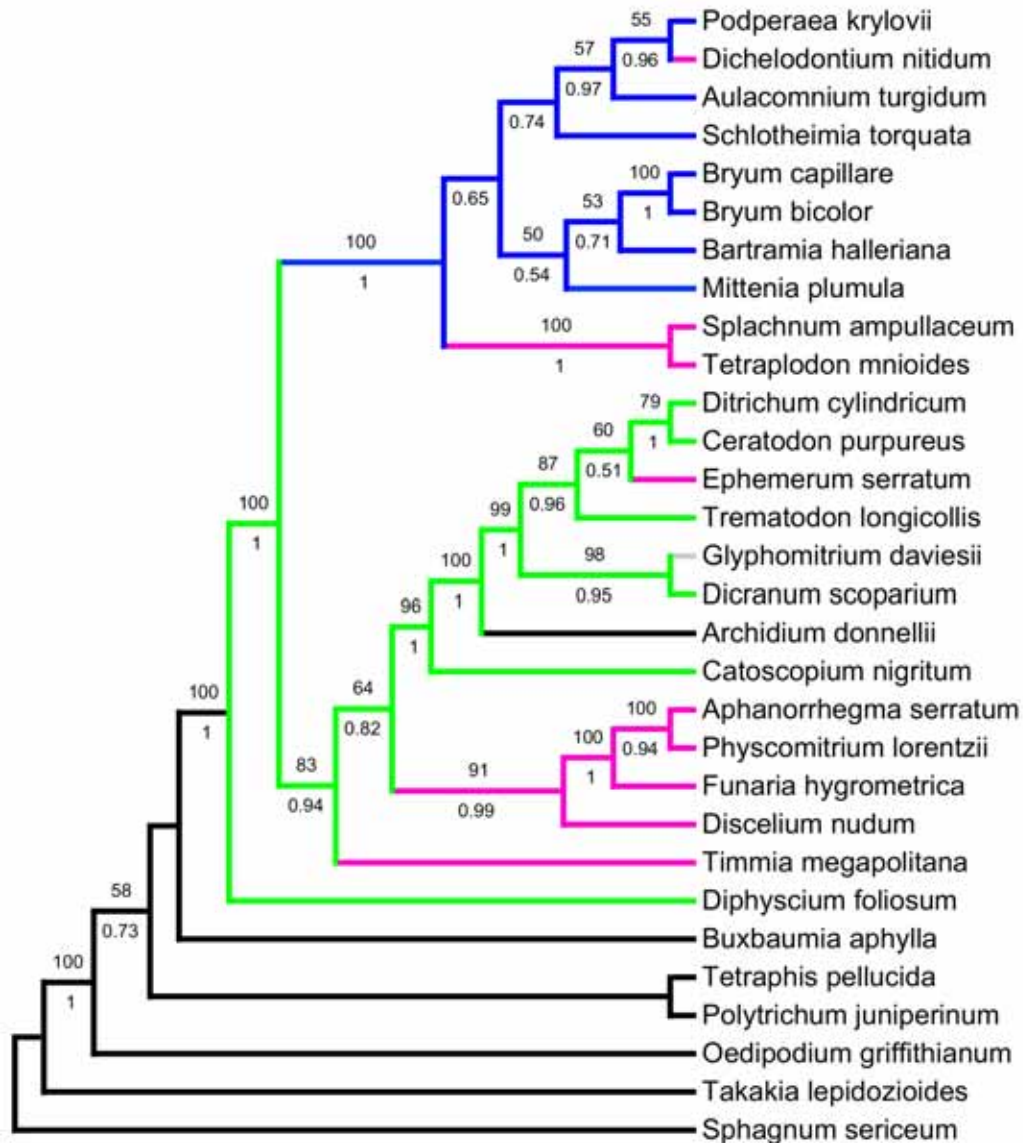


Fig. 12. The best RAxML likelihood tree obtained from the concatenated *rps4* and *nad5* sequences (data set 1), for the genera included in the peristome development studies (marked by color), supplemented with representatives of other families, not included in the morphological studies (those are without color marks). Posterior probabilities (>50) are shown below the branches while Bootstrap support (>50) is indicated above branches. 4:2:4-alternate pattern is attributed to *Mittenia* basing on Fig. 40 in Stone (1961). Pink color mark lineages to 4:2:4-opposite pattern, green to 4:2:3 pattern, blue to 4:2:4-alternate one. Families without arthrodoxous peristomes are in black.

duced one. The obvious cases of reduction in *Ephemerium*, *Tetraplodon*, *Splachnum* and *Dichelodontium* were mentioned, but then the question is raised, if the 'true dipolepeidous-opposite' mosses are so strongly different from them? Five orders belong now to this 'true dipolepeidous-opposite' group: Gigaspermales, Funariales, Disceliales, Encalyptales and Timmiales. Among them, Gigaspermales have no peristomes at all, Disceliales with a single species have a peristome which provides only slow and limited hygroscopic movements. Peristomes of Encalyptales are quite passive, because hygroscopic movements are not really needed under the cover of giant campanulate calyp-

tra, when many species apparently start spore release. Complex and hygroscopically active peristomes occur in two orders, Funariales and Timmiales, both with a single family. Moreover, in Funariaceae most taxa either lack, or have only poorly developed peristomes, so only within the one genus *Funaria*, albeit a widespread one, the dipolepeidous-opposite peristome functions in spore release, and again only in about a half of species it is fully developed. Timmiaceae is the only family where all species have perfectly hygroscopic and xerocastique peristomes, but these species are few, less than ten in the world (Tropicos, <http://www.tropicos.org/namesearch.aspx>).

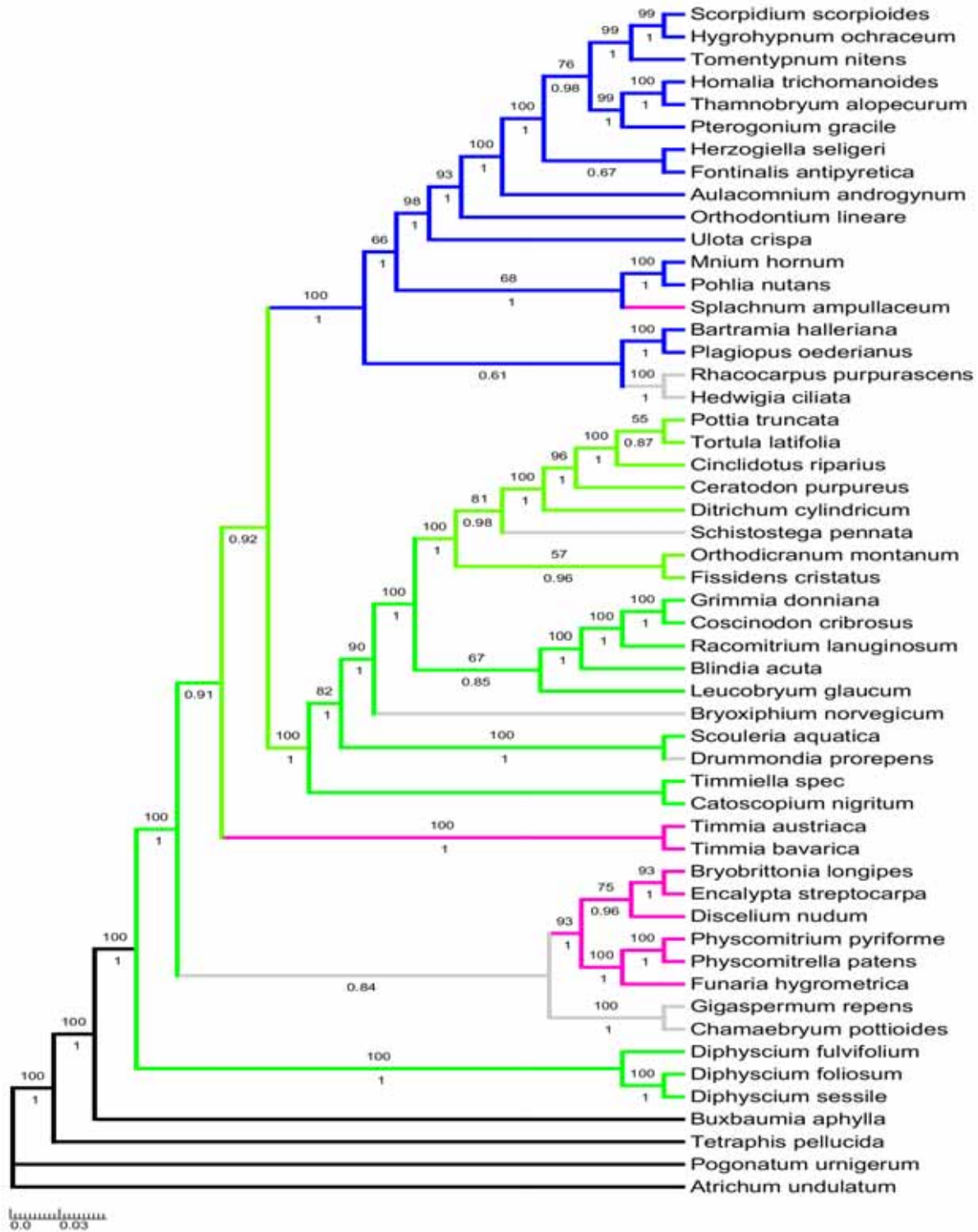


Fig. 13. The inferred maximum likelihood topology (RAxML) obtained from a concatenated data set of 7 loci (data set 2) spanning 4 region of the chondrom (*cob1420*, *nad2* with *nad2i156*, *nad5* with *nad5i753*, *nad5-nad4* intergenic spacer (IGS)) and three from the plastome (*rbcL*, *rps4*, *trnL* including a group I intron). Posterior probabilities (>50) are shown below the branches while Bootstrap support (>50) is indicated above branches. Pink color mark lineages to 4:2:4-opposite pattern, green to 4:2:3 pattern, blue to 4:2:4-alternate one. Families with nematodontous peristomes are in black, and lineages within arthrodontous mosses lacking peristomes in any families are in grey.

Further observations may confirm if the loss of unequal divisions at the transition from 2:2:1 to 4:2:2 is the main reason for peristome reduction among other moss groups. However the great role of asymmetric cell divisions in differentiation of plant body is well known (De Smet & Beeckman, 2011), thus relaxation of this pattern may naturally lead to the simplification or at least building of less constructively perfect morphology.

The position of *Catoscopium* in moss phylogeny is especially interesting: if its peristome development is based on 4:2:3 pattern, it should be considered as the most ancient moss with a more or less developed peristome involving asymmetric cell divisions for tooth formation, as the still phylogenetically earlier case of *Diphyscium* (Figs. 12 & 13) sharing this pattern does not develop any teeth. An interesting fact is also that *Catoscopium* retains an ability to keep a largely ‘unspecialized’ type of peristome development, easily shifting to the diplolepidous-alternate and the diplolepidous-opposite patterns (Fig. 10), quite justifying its position near the cross-road of moss evolution. The question remains why a shift to the haplolepidous peristome type occurred, *i.e.* pronouncing the endostome instead of the exostome (as in *Catoscopium*), which resulted in a major radiation of mosses.

#### ACKNOWLEDGEMENTS

We thank John Shaw for critical comments and a language check. We are grateful to Alfons Schäfer-Verwimp for sharing his specimen with us and to Markus Günther (TU Dresden) for SEM assistance. Special thanks are to Oleg Ivanov who suggested the idea of RGB-coding of peristome layers. Partial financial support by the Russian Foundation for Basic Researches, 13-04-01592 for MI and UN, by the Russian Science Foundation, 14-50-00029 for EI, and the German Research Foundation (DFG) for DQ (QU 153/3-1) is greatly appreciated.

#### LITERATURE CITED

- ALLEN, B.H. 1987. A systematic account of *Pulchrinodus inflatus* (Musci: Pterobryaceae), genus novum. – *New Zealand Journal of Botany* **25**: 335–342.
- BLOMQUIST, H.L. & L.L. ROBERTSON. 1941. The development of the peristome in *Aulacomnium heterostichum*. – *Bulletin of the Torrey Botanical Club* **65**: 569–584.
- BORSCH, T. & D. QUANDT. 2009. Mutational dynamics and phylogenetic utility of non-coding plastid DNA. – *Plant Systematics and Evolution* **282**: 169–199.
- BROTHERUS, V.F. 1924. Musci. – In: Engler, A. & K. Prantl (eds.). *Die Natürlichen Pflanzenfamilien*. 2, 10. Berlin: Duncker and Humblot: 143–478.
- BUCK, W.R. & B. GOFFINET. 2000. Morphology and classification of mosses. – In: Shaw, A. J. & B. Goffinet (eds.). *Bryophyte biology*. Cambridge University Press, Cambridge, UK: 71–123.
- BUCK, W.R., B. GOFFINET & A.J. SHAW. 2000. Testing morphological concepts of orders of pleurocarpous mosses (Bryophyta) using phylogenetic reconstructions based on trnL-trnF and rps4 sequences. – *Molecular Phylogenetics and Evolution* **16**: 180–198.
- BUDKE, J.M., C.S. JONES & B. GOFFINET. 2007. Development of the enigmatic peristome of *Timmia megapolitana* (Timmiaaceae; Bryophyta). – *American Journal of Botany* **94**(3): 460–467.
- COX, C.J., B. GOFFINET, N.J. WICKETT, S.B. BOLES & A.J. SHAW. 2010. Moss diversity: a molecular phylogenetic analysis of genera. – *Phytotaxa* **9**: 175–195.
- COX, C. J., B. GOFFINET, A.J. SHAW & S.B. BOLES. 2004. Phylogenetic relationships among the mosses based on heterogeneous Bayesian analysis of multiple genes from multiple genomic compartments. – *Systematic Botany* **29**: 234–250.
- CRUM, H.A. & L.E. ANDERSON. 1981. Mosses of Eastern North America. Volume 1. – Columbia University Press, New York, 1–663.
- DE SMET, I. & T. BEECKMAN. 2011. Asymmetric cell division in land plants and algae: the driving force for differentiation. – *Nature Reviews Molecular Cell Biology* **12**: 177–188. | doi:10.1038/nrm3064
- DEMIDOVA, E.E. & V.R. FILIN. 1994. False columella and spore release in *Tetraplodon angustatus* (Hedw.) Bruch et Schimp. in B. S. G. and T. mnioides (Hedw.) Bruch et Schimp. in B. S. G. (Musci: Splachnaceae). – *Arctoa* **3**: 1–6.
- EDWARDS, S.R. 1979. Taxonomic implications of cell patterns in haplolepidous moss peristomes. – In: Clarke, G.C.S. & J.G. Duckett (eds.). *Bryophyte systematics*. Academic Press, London, UK: 317–346.
- EDWARDS, S.R. 1984. Homologies and inter-relations of moss peristomes. – In: Schuster, R.M. (ed.) *New manual of bryology*, vol. 2. Hattori Botanical Laboratory, Nichinan, Japan: 658–695.
- ESTÉBANEZ, B., T. YAMAGUCHI & H. DEGUCHI. 2006. The development of an unusual haplolepidous peristome type: *Glyphomitrium humilimum*. – *Journal of the Hattori Botanical Laboratory* **100**: 77–87.
- EVANS, A.W. & H.D. HOOKER, jr. 1913. Development of the peristome in *Ceratodon purpureus*. – *Bulletin of the Torrey Botanical Club* **40**: 97–109.
- FREY, W. & M. STECH. 2009. Bryophyta (Musci, mosses). – In: Frey, W. (ed.). *Syllabus of plant families A. Engler's Syllabus der Pflanzenfamilien*. Part 3. Bryophytes and seedless vascular plants. 13th ed.. Gebr. Borntraeger Verlagsbuchhandlung, Stuttgart, Germany: 116–257.
- GOFFINET, B., W.R. BUCK & A.J. SHAW. 2009. Morphology, anatomy, and classification of the Bryophyta. – In: Goffinet, B. & A.J. Shaw (eds.). *Bryophyte biology*, 2nd edn. Cambridge: Cambridge University Press: 55–138.
- GOFFINET, B., J. SHAW, L.E. ANDERSON & B.D. MISHLER. 1999. Peristome development in mosses in relation to systematics and evolution. V. Diplolepidae: Orthotrichaceae. – *Bryologist* **102**: 581–594.
- GRIFFIN, D.I. & W. R. BUCK. 1989. Taxonomic and phylogenetic studies on the Bartramiaceae. – *Bryologist* **92**: 368–380.
- HUTTUNEN, S., N. BELL, V.K. BOBROVA, V. BUCHBENDER, W.R. BUCK, C.J. COX, B. GOFFINET, L. HEDENAS, B.-C. HO, M.S. IGNATOV, M. KRUG, O. KUZNETSOVA, I.A. MILYUTINA, A. NEWTON, S. OLSSON, L. POKORNY, J.A. SHAW, M. STECH, A. TROITSKY, A. VANDERPOORTEN & D. QUANDT. 2012. Disentangling knots of rapid evolution: origin and diversification of the moss order Hypnales. – *Journal of Bryology* **34**: 187–211.
- HUTTUNEN, S., S. OLSSON, V. BUCHBENDER, J. ENROTH, L. HEDENÄS & D. QUANDT. Phylogeny-based comparative methods question the adaptive nature of sporophytic specialisations (in mosses). – *PlosOne* **7**: e48268.
- HYVÖNEN, J., S. KOSKINEN, G.L.S. MERRILL, T.A. HEDDERSON & S. STENROOS. 2004. Phylogeny of the Polytrichales (Bryophyta) based on simultaneous analysis of molecular and morphological data. – *Molecular Phylogenetics and Evolution* **31**: 915–928.
- IGNATOV, M.S., O.M. AFONINA & E.A. IGNATOVA (eds.) 2006. Checklist of mosses of East Europe and North Asia. – *Arctoa* **15**: 1–130.
- IGNATOV, M.S., A.A. GARDINER, V.K. BOBROVA, I.A. MILYUTINA, S. HUTTUNEN & A.V. TROITSKY. 2007. On the relationships

- of mosses of the order Hypnales, with special reference to taxa traditionally classified in the Leskeaceae. – In: Newton, A.E. & R.S. Tangney (eds.). *Pleurocarpous mosses: systematics and evolution. Systematic Association, Special Volume 71*: 177–213.
- IGNATOV, M.S. & E.A. IGNATOVA. 2003. Moss flora of the Middle European Russia. Vol. 1: Sphagnaceae – Hedwigiaceae. – Moscow: KMK Sc. Press Ltd.: 1–608.
- INOUE, Y. & H. TSUBOTA. 2014. On the systematic position of the genus *Timmiella* (Dicranidae, Bryopsida) and its allied genera, with the description of a new family Timmiellaceae. – *Phytotaxa* **181**(3): 151–162.
- KELCHNER, S.A. 2000. The evolution of non-coding chloroplast DNA and its application in plant systematics. – *Annals of the Missouri Botanical Garden* **87**: 482–498.
- LIMPRICHT, K.G. 1895. Die Laubmoose Deutschlands, Oesterreichs und der Schweiz. 2. Abt. – *Eduard Kummer, Leipzig*.
- MAGILL, R.E. 1987. On the endostomial nature of the *Dichelodontium* (Ptychomniaceae) peristome. – *Memoirs of the New York Botanical Garden* **45**: 87–94.
- MURPHY, S.A. 1988. Development of the peristome of *Timmia megalopolitana* Hedw. – *M.S. thesis, University of Iowa, Ames, Iowa, USA*.
- NEWTON, A.E., C.J. COX, J.G. DUCKETT, J.A. WHEELER, B. GOFFINET, T.A.J. HEDDERSON & B.D. MISHLER. 2000. Evolution of the major moss lineages: phylogenetic analyses based on multiple gene sequences and morphology. – *Bryologist* **103**: 187–211.
- OLSSON, S., V. BUCHBENDER, J. ENROTH, L. HEDENÄS, S. HUTTUNEN & D. QUANDT. 2009. Phylogenetic analyses reveal high levels of polyphyly among pleurocarpous lineages as well as novel clades. – *Bryologist* **112**: 447–466.
- PODPERA, J. 1954. *Conspectus muscorum Europaeorum*. – Prague. *Czechoslovakian Academy*, 697 pp.
- QUANDT, D., N. BELL & M. STECH. 2007. Unravelling the knot: the Pulchrinodaceae fam. nov. (Bryales). – *Nova Hedwigia* **131**: 21–39.
- QUANDT, D., K. MÜLLER & S. HUTTUNEN. 2003. Characterisation of the chloroplast DNA *psbT-H* region and the influence of dyad symmetrical elements on phylogenetic reconstructions. – *Plant Biology* **5**: 400–410.
- RAMBAUT, A., M.A. SUCHARD, D. XIE & A.J. DRUMMOND. 2014. Tracer v1.6. – Available from <http://beast.bio.ed.ac.uk/Tracer>.
- RONQUIST, F., M. TESLENKO, P. VAN DER MARK, D.L. AYRES, A. DARLING, S. HÖHNA, B. LARGET, L. LIU, M.A. SUCHARD & J.P. HUELSENBECK. 2012. MRBAYES 3.2: Efficient Bayesian phylogenetic inference and model selection across a large model space. – *Systematic Biology* **61**: 539–542.
- REYNOLDS VAIZEY, J. 1888. On the anatomy and development of the sporogonium of the mosses. – *Journal of the Linnean Society* **24**: 262–285+PL.9–12.
- SAITO, S. 1956. Studies on the development of the peristome in Musci II. On the peristome in *Dicranum japonicum* Mitt. – *Botanical Magazine, Tokyo* **69**(812): 53–59.
- SAITO, S. & S. SHIMOZE. 1955. Studies on the development of the peristome in Musci I. On the peristome in *Bartramia crispula* Schimp. – *Botanical Magazine, Tokyo* **69**(812): 53–59.
- SCHWARTZ, O.M. 1994. The development of the peristome-forming layers in the Funariaceae. – *International Journal of Plant Science* **155**: 640–657.
- SCHIMPER, W.P. 1860. *Synopsis Muscorum Europeorum*. – E. Schweizerbart, Stuttgart, 733 pp.
- SHAW, J. 1985. The correlation between taxonomy and peristome structure in the Bryaceae. – *Journal of the Hattori Botanical Laboratory* **59**: 79–100.
- SHAW, J. & B.H. ALLEN. 1985 [1986]. Anatomy and morphology of the peristome in *Discelium nudum* (Musci: Disceciaceae). – *Bryologist* **88**: 263–267.
- SHAW, A.J. & L.E. ANDERSON. 1988. Peristome development in mosses in relation to systematics and evolution II. *Tetraphis pellucida* (Tetraphidaceae). – *American Journal of Botany* **75**: 1019–1032.
- SHAW, A.J., L.E. ANDERSON & B.D. MISHLER. 1987. Peristome development in mosses in relation to systematics and evolution I. *Diphyscium foliosum* (Diphysciaceae). – *Memoirs of the New York Botanical Garden* **45**: 55–70.
- SHAW, A.J., L.E. ANDERSON & B.D. MISHLER. 1989a. Peristome development in mosses in relation to systematics and evolution III. *Funaria hygrometrica*, *Bryum pseudocapillare*, and *B. bicolor*. – *Systematic Botany* **14**: 24–36.
- SHAW, A.J., L.E. ANDERSON & B.D. MISHLER. 1989b. Peristome development in mosses in relation to systematics and evolution IV. Haplloepideae: Ditrichaceae and Dicranaceae. – *Bryologist* **92**: 314–323.
- SHAW, A. J., C. J. COX, B. GOFFINET, W. R. BUCK & S. B. BOLES. 2003. Phylogenetic evidence of a rapid radiation of pleurocarpous mosses (Bryophyta). – *Evolution* **57**: 2226–2241.
- SHAW, J. & K. RENZAGLIA. 2004. Phylogeny and diversification of Bryophytes. – *American Journal of Botany* **91**(10): 1557–1581.
- SHAW, A.J. & H. ROBINSON. 1984. On the development, evolution, and function of peristome in mosses. – *Journal of the Hattori Botanical Laboratory* **57**: 319–335.
- SHAW, A.J., P. SZÖVÉNYI & B. SHAW. 2011. Bryophyte diversity and evolution: windows into the early evolution of land plants. – *American Journal of Botany* **98**(3): 352–369.
- SHIMAMURA, M. & H. DEGUCHI. 2008. Sporophyte anatomy of *Oedipodium griffithianum* (Oedipodiaceae). – In: Mohamed, H., B.B. Baki, A. Nasrullah-Boyce et al. (eds.). *Bryology in the New Millennium. Institute of Biological Sciences, University of Malaya, Kuala Lumpur, Malaysia*: 319–325.
- SNIDER, J.A. 1975a. A revision of the genus *Archidium* (Musci). – *Journal of the Hattori Botanical Laboratory* **39**: 105–201.
- SNIDER, J.A. 1975b. Sporophyte development in the genus *Archidium*. – *Journal of the Hattori Botanical Laboratory* **39**: 85–104.
- STAMATAKIS, A. 2014. RAxML Version 8: A tool for Phylogenetic Analysis and Post-Analysis of Large Phylogenies. – *Bioinformatics* **30**: 1312–1313.
- STÖVER, B.C. & K.F. MÜLLER. 2010. TreeGraph 2: Combining and visualizing evidence from different phylogenetic analyses. – *BMC Bioinformatics* **11**: 7.
- STECH, M., S.F. McDANIEL, R. HERNÁNDEZ-MAQUEDA, R.M. ROS, O. WERNER, J. MUÑOZ & D. QUANDT. 2012. Phylogeny of haplloepideous mosses – challenges and perspectives. – *Journal of Bryology* **34**(3): 173–186.
- STONE, I.G. 1961. The gametophore and sporophyte of *Mittenia plumula* (Mitt.) Lindb. – *Australian Journal of Botany* **9**: 124–151.
- TSUBOTA, H., E. DE LUNA, D. GONZÁLEZ, M.S. IGNATOV & H. DEGUCHI. 2004. Molecular phylogenetic and ordinal relationships based on analyses of a large-scale data set of 600 rbcL sequences of mosses. – *Hikobia* **14**: 149–170.
- WAHRMUND, U., D. QUANDT & V. KNOOP. 2010. The phylogeny of mosses – addressing open issues with a new mitochondrial locus: Group I intron *cob1420*. – *Molecular Phylogenetics and Evolution* **54**: 417–426.
- WENDEROTH, H. 1931. Beiträge zur Kenntnis des Sporophyten von *Polypodium juniperinum*. Willdenow. – *Planta* **14**: 244–385.

Appendix 1. Sequences used for a small taxon subset consisting only of genera used for peristome development studies supplemented with eperistomate *Sphagnum* and *Takakia* (data set 1).

<i>Species</i>	<i>GenBank accessions</i>		<i>Reference for anatomy study</i>
	<i>nad5 with nad5i753</i>	<i>rps4</i>	
<i>Sphagnum sericeum</i>	AY309571	AY309717	
<i>Takakia lepidozoides</i>	AJ291553	AB299143	
<i>Oedipodium griffithianum</i>	AY312880	AF306968	Shimamura & Deguchi, 2008
<i>Polytrichum juniperinum</i>	GU56958	EU927342	Reynolds Vaizey, 1888 ( <i>Polytrichum formosum</i> ) and Wenderoth, 1931 ( <i>P. juniperinum</i> ).
<i>Buxbaumia aphylla</i>	AY312872	AY137677	
<i>Tetraphis pellucida</i>	AJ224855	AY908021	Shaw & Anderson, 1988
<i>Diphyscium foliosum</i>	AY312874	AF223034	Shaw <i>et al.</i> , 1987
<i>Aphanorrhagma serratum</i>	AY908931	AF223047	Schwartz, 1994
<i>Funaria hygrometrica</i>	Z98959	JN088980	Shaw <i>et al.</i> , 1989a Schwartz, 1994 ( <i>F. hygrometrica</i> and <i>F. flavicans</i> )
<i>Physcomitrium lorentzii</i>	AY908933	AF223046	Schwartz, 1994 ( <i>P. pyriforme</i> )
<i>Discelium nudum</i>	AY908956	AF223063	Shaw & Allen, 1985
<i>Timmia megapolitana</i>	AY312890	AF478287	Budke <i>et al.</i> , 2007
<i>Ephemerum serratum</i>	AY908848	AY908061	Schwartz, 1994
<i>Archidium donnellii</i>	AY908972	AF223054	Snider, 1975b ( <i>A. ochioense</i> )
<i>Ditrichum cylindricum</i>	AJ291559	AY908125	Shaw <i>et al.</i> , 1989b ( <i>D. lineare</i> and <i>D. pallidum</i> )
<i>Mittenia plumula</i>	N.A.	AF306999	Stone, 1961
<i>Trematodon longicollis</i>	N.A.	AY908087	Shaw <i>et al.</i> , 1989b
<i>Catoscopium nigratum</i>	AY908927	AF307001	present paper
<i>Ceratodon purpureus</i>	AY908862	AB848717	Evans & Hooker, 1913
<i>Dicranum scoparium</i> <sup>1</sup>	AY908884	AF234158	Shaw <i>et al.</i> , 1989b <sup>1</sup>
<i>Glyphomitrium daviesii</i>	AY908895	N.A.	Estébanez <i>et al.</i> , 2006 ( <i>G. humillimum</i> )
<i>Tetraplodon mnioides</i>	AY908376	AY499644	Schwartz, 1994
<i>Splachnum ampullaceum</i>	EU095308	AY499621	Schwartz, 1994
<i>Bartramia halleriana</i>	Z98961	AF265358	Saito & Shimoze, 1955 ( <i>B. crispula</i> )
<i>Bryum bicolor</i>	DQ640119	DQ294323	Shaw <i>et al.</i> , 1989a
<i>Bryum capillare</i>	DQ640122	JF277331	Shaw <i>et al.</i> , 1989a ( <i>B. pseudocapillare</i> )
<i>Podperaea krylowii</i>	N.A.	KT388714	present paper
<i>Dichelodontium nitidum</i>	AY452347	AY449664	Magill, 1987
<i>Schlotheimia torquata</i>	AY618409	AY908005	Goffinet <i>et al.</i> , 1999
<i>Aulacomnium turgidum</i>	AY312869	AF023809	Blomquist & Robertson. 1941 ( <i>A. heterostichum</i> )

<sup>1</sup> – similar anatomy has been found for *D. condensatum* and *D. rhabdocarpum* (Shaw *et al.*, 1989b) and *D. japonicum* (Saito, 1956).

Appendix 2. Accession numbers for the sequences used to compile the bryophyte backbone data set (data set 2, adopted from Wahrmond et

Taxonomy	Species	cobi420	nad2 with nad21156	nad5 with nad5i753	nad5- nad4 IGS	rbcL	rps4	trnL G1
Polytrichopsida: Polytrichaceae	<i>Atrichum undulatum</i>	FJ870696	AJ299527	AJ001229	EU095269	AY118236	AY137681	AF545002
	<i>Pogonatum urnigerum</i>	FJ870699	AJ299528	AJ291554	EU095272	AF478206	AF478258	GU569719
Tetraphidopsida: Tetraphidaceae	<i>Tetraphis pellucida</i>	FJ870700	AJ299529	AJ224855	EU095273	<i>P. perichaetiale</i> AF478203	AF306954	AF231908.
	<b>Bryopsida</b>							
Buxbaumiales: Buxbaumiaceae	<i>Buxbaumia aphylla</i>	FJ870701	AJ299531	AJ291555	EU095274	AF478212	AF231897	AF478299
Diphysciales: Diphysciaceae	<i>Diphyscium sessile</i>	FJ870702	AJ299530	Z98972	EU095275	n.a.	n.a.	n.a.
	<i>Diphyscium foliosum</i>	n.a.	n.a.	AY312874	n.a.	AY312928	AF223034	AF229891
	<i>Diphyscium fulvifolium</i>	n.a.	n.a.	JX241614	n.a.	AF478222	AF478266	AF478310
Timmiales: Timmiaceae	<i>Timmia austriaca</i>	FJ870703	FJ870755	FJ870748	FJ870748	AJ275185	AF223035	DQ397165
	<i>Timmia bavarica</i>	FJ870704	AJ299532	AJ622820	EU095276	DQ778619	AF222902	AF435351
Gigaspermiales: Gigaspermaceae	<i>Chamaebryum pottioides</i>	FJ870706	FJ870757	AY908983	FJ870750	FJ870761	AF223051	AF229908
	<i>Gigaspermum repens</i>	FJ870707	FJ870758	AY908974	FJ870751	FJ870762	AF231064	AF229906
Encalyptales: Encalyptaceae	<i>Bryobrittonia longipes</i>	FJ870709	EU095311	AY908790	EU095277	AJ275168	AF023778	AF023718
	<i>Encalypta streptocarpa</i>	FJ870710	AJ299533	AJ291556	EU095278	AF478239	AF478282	AF478325
	<i>Funaria hygrometrica</i>	FJ870711	AJ299534	Z98959	EU095279	AF005513	AF023776	EU1866538
	<i>Physcomitrella patens</i>	NC007945	AJ299535	Z98960	DQ098674	AP005672	NC005087	EU1866539
	<i>Physcomitrium pyriforme</i>	FJ870712	EU095312	AY908933	EU095280	EU095319	AF223045	AF229902
Discellaceae	<i>Discellium nudum</i>	FJ870713	EU095313	<i>P. lorentzii</i> AY908956	EU095281	EU095320	AF223063	AF229920
	Catoscopiales: Catoscopiaceae	<i>Catoscopium nigratum</i>	FJ870735	AY908927	FJ870753	FJ870764	AF307001	EU186545
Scouleriales: Drummondiales		<i>Drummondia proropens</i>	FJ870714	AY908926	EU095282	AF232697	AF306977	AF229895
Scouleriales: Scouleriaceae	<i>Scouleria aquatica</i>	n.a.	n.a.	<i>D. obtusifolia</i> AY312887	n.a.	AF226822	AF306984	AF023723
	<i>Bryoxiphium norvegicum</i>	n.a.	n.a.	AY908957	n.a.	AB194720	AY908092	AF229894
	Grimmiales: Grimmiaceae	<i>Grimmia (Coscinodon) cribrusosus</i>	FJ870715	AY908918	EU095283	AB125575	AJ553978	DQ399642
Grimmiales: Grimmiaceae	<i>Grimmia donniana</i>	FJ870716	EU095315	<i>C. calyptratus</i> AY908919	EU095284	AF231305	AF222900	AJ879718
Grimmiales: Grimmiaceae	<i>Racomitrium lanuginosum</i>	FJ870717	AJ299542	<i>G. plagiopodia</i> AJ291561	EU095285	G. pulvinata AB125582	AJ553982	EU246926
Grimmiales: Seligeriaceae	<i>Blindia acuta</i>	FJ870718	EU095316	AY908928	EU095286	<i>R. japonicum</i> AF478232	AF478278	R. elongatum AF023721
Dicranales: Dicranaceae	<i>Orthodicranum montanum</i>	FJ870719	AJ299537	AJ291558	EU095287	<i>B. magellanica</i> AF231311	AF231288	AF129589

## Appendix 2. (continued).

Dicranales: Fissidentaceae	<i>Fissidens cristatus</i>	FJ870720	AJ299541	Z98954	DQ098675	O. fulvum DQ463104	O. fulvum DQ463123	AF135104
Dicranales: Ditrichaceae	<i>Ceratodon purpureus</i> <i>Ditrichum cylindricum</i>	FJ870721 FJ870722	AJ299538 AJ299539	Z98955 AJ291559	EU095288 EU095289	F. taxifolius EU095321	F. taxifolius AJ554004	AB848718 AF231248
Dicranales: Schistostegaceae	<i>Schistostega pennata</i>	FJ870723	AJ299546	AJ224856	EU095290	D. pallidum AF631206	D. pallidum AF265359	LN828226
Dicranales: Leucobryaceae	<i>Leucobryum glaucum</i>	FJ870724	AJ299540	AJ291560	EU095291	AB124788	AJ554003	AF135083
Pottiales: Pottiaceae	<i>Pottia truncata</i>	FJ870725	AJ299543	Z98957	EU095292	AB125592	AF480987	AF135112
Pottiales: Pottiaceae	<i>Syntrichia (Tottrula) latifolia</i>	FJ870727	AJ299544	AJ291562	EU095294	P. intermedia AF226823	P. pallida AF481041	AF135108
Pottiales: Timmiellaceae	<i>Timmiella spec.</i>	FJ870726	EU095317	AY908958	EU095293	T. obtusissima AF478236	T. muralis AY908163	T. muralis AF231173
Pottiales: Cinclidoteaceae	<i>Cinclidotus riparius</i>	FJ870728	AJ299545	AJ291563	EU095295	T. crassinervis AF231079	T. anomala AF480975	T. crassinervis EU186654
Splachnales: Splachnaceae	<i>Splachnum ampullaceum</i>	FJ870729	<b>Bryidae</b>	EU095308	EU095296	C. mucronatus AF231071	C. fontinaloides AJ251308	C. nigricans AF215899
Orthotrichales: Orthotrichaceae	<i>Ulota crispa</i>	FJ870730	AJ299553	AJ291568	EU095297	AY631208	AY618370	EU186657
Hedwigiales: Hedwigiaceae	<i>Hedwigia ciliata</i>	FJ870731	AJ299554	Z98966	EU095298	AF005517	U. hutchinsiae AF478289	AF478336
Hedwigiales: Rhacocarpaceae	<i>Rhacocarpus purascens</i>	FJ870732	AJ299555	Z98967	EU095299	AJ275171	AF023815	HF536608
Bartramiales: Bartramiaceae	<i>Bartramia halleriana</i>	FJ870733	AJ299547	Z98961	EU095300	AF231090	AF265358	AY532395
Bartramiales: Bartramiaceae	<i>Plagiopus oederi</i>	FJ870734	AJ299548	Z98962	EU095301	DQ481540	AF023833	AF023757
Bryales: Mniaceae	<i>Mnium hornum</i>	FJ870736	AJ299552	AJ291567	EU095302	AF226820	AF023796	AF231177
Bryales: Mielichhoferiaceae	<i>Pohlia nutans</i>	FJ870737	AJ299550	AJ291565	EU095303	AJ275175	AF023795	DQ108957
Rhizogoniales: Aulacomniaceae	<i>Aulacomnium androgynum</i>	FJ870738	AJ299549	AJ291564	EU095304	P. cruda AJ275180	P. cruda AF023809	AF023729
Rhizogoniales: Orthodontiaceae	<i>Orthodontium lineare</i>	FJ870739	AJ299551	AJ291566	EU095305	A. turgidum AJ275174	A. turgidum AF023800	EU186558
Hypnales: Plagiotheciaceae	<i>Herzogiella seligeri</i>	FJ870740	AJ299561	AJ291573	DQ098681	EU095322	AF469815	AF472453
Hypnales: Fontinalaceae	<i>Fontinalis antipyretica</i>	FJ870741	AJ299558	AJ291570	EU095306	AB050949	AF023817	AF023771
Hypnales: Amblystegiaceae s.l.	<i>Hygrohypnum ochraceum</i>	FJ870742	AJ299562	AJ291574	DQ098679	EU095323	AY908620	AY012571
Hypnales: Amblystegiaceae s.l.	<i>Scorpidium scorpioides</i>	FJ870743	AJ299563	AJ291575	DQ098680	EU095324	AY908584	AY626014
Hypnales: Amblystegiaceae s.l.	<i>Tomentypnum nitens</i>	FJ870744	AJ299560	AJ291572	DQ098677	AB024676	AY908567	AY009854
Hypnales: Leucodontaceae	<i>Pterogonium gracile</i>	FJ870745	AJ299556	Z98968	EU095307	AY631194	T. falcatulum AY907970	HE717062
Hypnales: Neckeraeae	<i>Homalia trichomanoides</i>	FJ870746	AJ299557	AJ291569	DQ098683	EU095325	AY908276	AM990385
Hypnales: Neckeraeae	<i>Thamnobryum alopecurum</i>	FJ870747	AJ299559	AJ291571	DQ098678	AY532392	AF023834	AY010287